

## Neutron Capture Measurements and Resonance Parameters of Gadolinium

Y.-R. Kang and M. W. Lee

*Dongnam Institute of Radiological and Medical Sciences, Research Center  
Busan 619-953, Korea*

G. N. Kim\*

*Kyungpook National University, Department of Physics  
Daegu 702-701, Korea*

T.-I. Ro

*Dong-A University, Department of Physics  
Busan 604-714, Korea*

Y. Danon and D. Williams

*Rensselaer Polytechnic Institute, Department of Mechanical, Aerospace, and Nuclear Engineering  
Troy, New York 12180-3590*

and

G. Leinweber, R. C. Block, D. P. Barry, and M. J. Rapp

*Bechtel Marine Propulsion Corporation, Knolls Atomic Power Laboratory  
P.O. Box 1072, Schenectady, New York 12301*

*Received June 6, 2014*

*Accepted July 15, 2014*

<http://dx.doi.org/10.13182/NSE14-80>

**Abstract**—Neutron capture measurements were performed with the time-of-flight method at the Gaerttner LINAC Center at Rensselaer Polytechnic Institute (RPI) using isotopically enriched gadolinium (Gd) samples ( $^{155}\text{Gd}$ ,  $^{156}\text{Gd}$ ,  $^{157}\text{Gd}$ ,  $^{158}\text{Gd}$ , and  $^{160}\text{Gd}$ ). The neutron capture measurements were made at the 25-m flight station with a 16-segment sodium iodide multiplicity detector. After the data were collected and reduced to capture yields, resonance parameters were obtained by a combined fitting of the neutron capture data for five enriched Gd isotopes and one natural Gd sample using the multilevel R-matrix Bayesian code SAMMY. A table of resonance parameters and their uncertainties is presented. We observed 2, 169, 96, and 1 new resonances in  $^{154}\text{Gd}$ ,  $^{155}\text{Gd}$ ,  $^{157}\text{Gd}$ , and  $^{158}\text{Gd}$  isotopes, respectively. Resonances in the ENDF/B-VII.0 evaluation that were not observed in the current experiment and could not be traced to a literature reference were removed. This includes 11 resonances from the  $^{156}\text{Gd}$  isotope, 1 resonance from  $^{157}\text{Gd}$ , 1 resonance from  $^{158}\text{Gd}$ , and 6 resonances from the  $^{160}\text{Gd}$  isotope.

---

\*E-mail: gnkim@knu.ac.kr

The resulting resonance parameters were used to calculate the capture resonance integrals in the energy region from 0.5 eV to 20 MeV and were compared to calculations obtained when using the resonance parameters from ENDF/B-VII.0 and previous RPI results. The present parameters gave a resonance integral value of  $395 \pm 2$  b, which is  $\sim 0.8\%$  higher and  $\sim 1.7\%$  lower than that obtained with the ENDF/B-VII.0 parameters and with the previous RPI parameters, respectively.

## I. INTRODUCTION

The stable isotopes of gadolinium (Gd) are significant fission products in fast reactors.<sup>1</sup> A major portion of neutron capture cross sections of natural Gd is due to <sup>155</sup>Gd and <sup>157</sup>Gd. Their capture cross sections and resonance parameters in the wider energy range are important in the design of reactors, as well as in nuclear and astrophysics studies.<sup>2</sup> Accurate knowledge of the neutron cross sections and the resonance parameters for Gd isotopes are of importance to the calculation of reactor characteristics when Gd is used as a burnable poison in commercial light water reactors. The capture cross section is also important to examine the Gd isotopes as a control material for fast reactors.<sup>3</sup>

Neutron capture experiments on Gd isotopes were performed at the electron linear accelerator (LINAC) facility of the Rensselaer Polytechnic Institute (RPI) in the neutron energy region from 10 eV to 1 keV. Resonance parameters were extracted by fitting the neutron capture data using the SAMMY multilevel R-matrix Bayesian code.<sup>4</sup> The default formalism for the SAMMY code is the Reich-Moore approximation, which is based on the idea that capture channels behave quite differently from particle channels.

Most of the strong resonances occur in <sup>155</sup>Gd and <sup>157</sup>Gd isotopes. In these two isotopes, ENDF/B-VII.0 resonance parameters are based on a few experiments, particularly Mughabghab and Chrien,<sup>5</sup> Simpson,<sup>6</sup> Møller et al.,<sup>7</sup> and Fricke et al.<sup>8</sup> Recently, the resonance parameters for <sup>155</sup>Gd were obtained from capture experiments with the DANCE calorimeter at the Los Alamos Neutron Science Center (LANSCE) in the neutron energy region from 1 eV to 200 eV (Ref. 9). The other high-abundance isotopes, <sup>156</sup>Gd, <sup>158</sup>Gd, and <sup>160</sup>Gd, have few resonances, and resonance parameters for <sup>158</sup>Gd and <sup>160</sup>Gd come from Mughabghab and Chrien<sup>5</sup> and Rahn et al.<sup>10</sup> The less abundant isotopes are <sup>152</sup>Gd and <sup>154</sup>Gd, which have a natural abundance of 0.2% and 2.1%, respectively. The resonance parameters for <sup>152</sup>Gd and <sup>154</sup>Gd come from Rahn et al.,<sup>10</sup> Anufriev et al.,<sup>11</sup> and Macklin.<sup>12</sup> Many other authors contributed observed resonance energies and/or spin assignments for resonances

energies above 148 eV including Belyaev et al.,<sup>13</sup> Karzhavina et al.,<sup>14,15</sup> and Asghar et al.<sup>16</sup> Finally, Leinweber et al.<sup>17</sup> measured resonance parameters of all naturally occurring Gd isotopes at the RPI LINAC facility in the neutron energy region from thermal to 300 eV.

## II. EXPERIMENTAL SETUP

### II.A. Pulsed Neutrons at RPI

Pulses of neutrons are generated via photoneutron reactions when an  $\sim 57$ -MeV electron beam from the RPI LINAC impinges on a water-cooled tantalum target. Table I gives some details of the experimental conditions including neutron target, overlap filter, pulse repetition rate, flight path length, and channel widths. Descriptions of the water-cooled tantalum target,<sup>18,19</sup> the capture detector,<sup>20,21</sup> and the data acquisition system<sup>20,22</sup> are given in detail elsewhere, so only a brief description is given in the present paper.

The geometry of the bare-bounce neutron target<sup>19</sup> (BBT) used for this measurement is unique in that the tantalum plates are mounted off the neutron beam axis. A 2.5-cm-thick polyethylene moderator is mounted adjacent to the tantalum plates and centered on the neutron beam axis. The moderator effectively slows down the fast neutrons generated in the target through collisions with hydrogen and emits the neutrons at a lower energy. These moderated neutrons are then collimated as they drift down an evacuated flight tube to the sample and detector. In order to remove low-energy neutrons from previous pulses, a 0.397-cm-thick <sup>10</sup>B<sub>4</sub>C overlap filter was inserted in the neutron beamline.

The neutron energy for a detected event is determined from the flight time of the neutron using the time-of-flight (TOF) technique and from the precise knowledge of the flight path length. The TOF analyzer used in the experiments was a multihit TOF clock (P7889, Fast ComTec.). The P7889 clock was operating with a 12.8-ns channel width and a total of 328125 channels. It operates as a single-start/multiple-stop device; i.e., a single LINAC burst initiates a countdown cycle,

TABLE I  
Experimental Conditions for Gd Capture Measurements

Neutron Producing Target	Overlap Filter	Average Beam Current ( $\mu$ A)	Beam Energy (MeV)	Pulse Width (ns)	Channel Width (ns)	Pulse Repetition Rate (pulse/s)	Flight Path Length (m)
BBT (Ref. 19)	Boron carbide	17.3	57	18	12.8	225	$25.569 \pm 0.006$

during which any number of detected events cause the analyzer to record an event. The TOF analyzer has no dead time between time bins to record each event. The overall dead time of the signal-processing electronics was set at 1.125  $\mu\text{s}$  for capture measurements. During operation of the experiment, data were transferred from the TOF analyzer to the computer memory via direct memory access. The data-taking software is completely menu driven and controls the sample changer, sorts the data into individual spectra, and provides online display of the data being accumulated. Descriptions of the data-taking computer system, data file structure, and data-reduction process are available in Ref. 23.

### II.B. Capture Detector

Neutron capture measurements were performed using a capture detector system, which is located at the 25-m flight station of the RPI LINAC. The capture detector<sup>20–22</sup> is a multiplicity-type scintillation gamma detector containing 20  $\ell$  of NaI(Tl) divided into 16 optically isolated segments, which forms a 30.5-cm-diameter  $\times$  30.5-cm-high right circular cylinder with an 8.9-cm through hole along its axis. The cylinder is split across its axis into two rings, with each ring divided into eight equal pie-shaped segments. Each segment is hermetically sealed in an aluminum can and is connected to a photomultiplier tube. The neutron beam was collimated to a diameter of 4.76 cm. Neutrons that scatter from the sample are absorbed by a 1.0-cm-thick hollow cylindrical liner fabricated of 99.4 wt%  $^{10}\text{B}$  carbide ceramic to reduce the number of scattered neutrons reaching the detector. The detector system discriminates against the 478-keV gamma ray from  $^{10}\text{B}(n;\alpha,\gamma)$  reactions. The capture detector is surrounded by a 15-cm-thick, 7260-kg lead shield to reduce ambient background signals. The capture detector used for the present experiment was located at the east beam tube at a flight path of  $25.569 \pm 0.006$  m from the BBT (Ref. 19). The flight path length was determined from measurements of precisely known  $^{238}\text{U}$  resonances.

The efficiency of detecting a capture event varies with the number and energy of gammas emitted in a capture event. The efficiency of detecting a single 2-MeV gamma

ray is  $\sim 75\%$  (Ref. 23). For capture in Gd where typically three to four gamma rays are emitted per capture, the efficiency is typically in excess of 95%. Thus, the capture efficiency is assumed to be the same for all Gd isotopes.

### II.C. Samples

In order to avoid the hydroscopic property of oxide power samples, five isotopically enriched Gd metallic samples were used. Two elemental Gd samples with different thicknesses were also used. The isotopic contents of the Gd samples used in the experiments are listed in Table II. The purity of elemental metallic samples was 99.8%. The isotopic abundances of the elemental sample were taken from Ref. 24. The only significant contaminant in the elemental sample was tantalum with a manufacturer-specified content of  $<0.1\%$ .

Three of the Gd isotopic samples ( $^{155}\text{Gd}$ ,  $^{156}\text{Gd}$ , and  $^{160}\text{Gd}$ ) were metallic disks with diameters of  $\sim 18$  mm and with thicknesses of  $\sim 0.1$  mm. Two Gd isotopic samples ( $^{157}\text{Gd}$  and  $^{158}\text{Gd}$ ) were metallic rectangular plates with sizes of  $15.22 \times 15.48$  mm for  $^{157}\text{Gd}$  and  $15.35 \times 15.14$  mm for  $^{158}\text{Gd}$  and with thicknesses of  $\sim 0.2$  mm. The characteristic details of the Gd samples are given in Table III. The uncertainties in thickness of samples were propagated from multiple measurements of the sample dimensions. The diameter and length measurements are the dominant component of the uncertainties. All samples were mounted in aluminum sample cans. The thickness of aluminum on each of the front and rear faces of each sample was 0.38 mm. The influence of these sample cans, as well as all background, was measured by including empty sample cans in the capture measurements. In order to measure the flight path length and to calibrate the neutron energy, a  $^{238}\text{U}$  sample was also measured.

Samples were precisely positioned at the center of the capture detector by a computer-controlled sample changer. The sample changer accommodated up to eight samples and moved them into the beam one at a time. These included five Gd isotopes, an elemental Gd sample, a  $^{238}\text{U}$  sample for energy calibration, and one empty sample holder for background evaluation.

TABLE II  
Isotopic Compositions of Gd Samples

Sample	Isotopic Composition (%)						
	$^{152}\text{Gd}$	$^{154}\text{Gd}$	$^{155}\text{Gd}$	$^{156}\text{Gd}$	$^{157}\text{Gd}$	$^{158}\text{Gd}$	$^{160}\text{Gd}$
$^{155}\text{Gd}$	0.04	$0.64 \pm 0.02$	$91.74 \pm 0.10$	$5.11 \pm 0.10$	$1.12 \pm 0.05$	$0.94 \pm 0.05$	$0.41 \pm 0.02$
$^{156}\text{Gd}$	$<0.01$	$0.11 \pm 0.01$	$1.96 \pm 0.02$	$93.79 \pm 0.03$	$2.53 \pm 0.02$	$1.20 \pm 0.02$	$0.41 \pm 0.02$
$^{157}\text{Gd}$	$<0.02$	$0.16 \pm 0.01$	$0.81 \pm 0.02$	$2.21 \pm 0.03$	$90.96 \pm 0.08$	$5.08 \pm 0.05$	$0.80 \pm 0.02$
$^{158}\text{Gd}$	$<0.1$	$<0.1$	$0.96 \pm 0.05$	$1.70 \pm 0.05$	$3.56 \pm 0.05$	$92.00 \pm 0.10$	$1.82 \pm 0.05$
$^{160}\text{Gd}$	$<0.01$	$0.02 \pm 0.00$	$0.18 \pm 0.01$	$0.32 \pm 0.02$	$0.43 \pm 0.02$	$0.93 \pm 0.02$	$98.12 \pm 0.05$
<i>nat</i> Gd	0.20	2.18	14.80	20.47	15.65	24.84	21.86

TABLE III  
Characteristics of Gd Samples

Sample	Atomic Weight	Mass (mg)	Thickness (mm)	Area (mm <sup>2</sup> )	Atoms/b
<sup>155</sup> Gd	$155.0 \pm 0.3$	$203.3 \pm 0.2$	$0.109 \pm 0.003$	$256 \pm 1$	$3.08 \times 10^{-4} \pm 1 \times 10^{-6}$
<sup>156</sup> Gd	$156.0 \pm 0.1$	$197.7 \pm 0.2$	$0.106 \pm 0.003$	$258 \pm 1$	$2.96 \times 10^{-4} \pm 2 \times 10^{-6}$
<sup>157</sup> Gd	$156.9 \pm 0.2$	$357.5 \pm 0.2$	$0.205 \pm 0.003$	$236 \pm 6$	$5.82 \times 10^{-4} \pm 14 \times 10^{-6}$
<sup>158</sup> Gd	$157.8 \pm 0.2$	$353.0 \pm 0.2$	$0.209 \pm 0.005$	$232 \pm 7$	$5.80 \times 10^{-4} \pm 16 \times 10^{-6}$
<sup>160</sup> Gd	$159.9 \pm 0.1$	$193.5 \pm 0.2$	$0.104 \pm 0.003$	$258 \pm 2$	$2.82 \times 10^{-4} \pm 2 \times 10^{-6}$
<i>nat</i> Gd <sup>a</sup>			0.254		$7.806 \times 10^{-4} \pm 0.4 \times 10^{-6}$
<sup>238</sup> U <sup>a</sup>		$18234.7 \pm 0.5$	0.493		$2.34 \times 10^{-3} \pm 2 \times 10^{-5}$

<sup>a</sup>Data taken from Ref. 17.

### III. DATA REDUCTION

The data-taking and data-reduction techniques that were used for this experiment are described in Ref. 23. For each sample, 16 TOF spectra with 328125 channels were measured; each of the 16 spectra represented a different observed gamma multiplicity. A minimum of 100-keV gamma energy was required in a detector segment to be counted. Data were recorded as capture events only if the total energy deposited in all 16 segments exceeded 1 MeV. The data were recorded as scattering events if the total deposited gamma-ray energy fell between 360 to 600 keV. This scattering energy region contains the 478-keV gamma ray emitted from the  $(n;\alpha,\gamma)$  reaction in the <sup>10</sup>B<sub>4</sub>C annular detector liner.

The large amount of TOF data collected in each capture measurement was subjected to statistical integrity checks to verify the stability of the electron LINAC, the capture detector, and associated beam monitors. The data were recorded in 398 files each containing data taken on all samples for a total time of  $\sim 54$  h. Any data that failed the integrity test were eliminated. Next, the data were dead-time corrected, normalized to beam monitors, and summed. The background was determined using normalized data measured with an empty aluminum sample holder mounted on the sample changer. This background was subtracted from the normalized and summed capture spectra. The 16 individual capture spectra were then summed into a single total spectrum.

Processed TOF data are expressed as capture yield. The capture yield is defined as the number of neutron captures per neutron incident on the sample. Therefore, in addition to the Gd sample data, another set of data was needed to determine the energy profile of the neutron flux. The capture yield  $Y_i$  in TOF channel  $i$  was calculated by

$$Y_i = \frac{C_i - B_i}{K\phi_{smi}} , \quad (1)$$

where

$C_i$  = dead-time–corrected and monitor-normalized counting rate of the sample measurement

$B_i$  = dead-time–corrected and monitor-normalized background counting rate

$K$  = product of the flux normalization factor and efficiency

$\phi_{smi}$  = smoothed, background-subtracted, and monitor-normalized neutron flux.

The incident neutron flux shape was determined by mounting a 2.54-mm-thick, 97.9 wt%–enriched <sup>10</sup>B<sub>4</sub>C sample in the sample changer and adjusting the total energy threshold to record the 478-keV gamma rays from neutron absorption in <sup>10</sup>B. A <sup>10</sup>B<sub>4</sub>C sample was used since it has high absorption and smooth cross section. The measured <sup>10</sup>B<sub>4</sub>C data and a correction for the neutron scattering and absorption in the <sup>10</sup>B<sub>4</sub>C were used to determine the neutron flux shape. These flux data gave the shape of the neutron beam flux but not its magnitude. The flux was smoothed by averaging adjacent points. The yield was normalized to the transmission parameters obtained from RPI data<sup>17</sup> using the SAMMY fit.

Background was not fitted during the SAMMY analysis. Background was measured using an empty sample holder and was subtracted from all samples. The measured flux shape is usually normalized directly to a saturated capture resonance. However, this was not possible in this experiment because there were no saturated resonances in any of the Gd isotopes; instead, the capture data were normalized using SAMMY to the previous RPI transmission data<sup>17</sup> at resonance energies listed in Table IV.

This capture yield and its associated statistical uncertainty were used as input parameters for the SAMMY code<sup>4</sup> that extracted the neutron resonance parameters. Capture data were not used below 10 eV due to excessive background.

### IV. DATA ANALYSIS

Resonance parameters, neutron width  $\Gamma_n$ , radiation width  $\Gamma_\gamma$ , and resonance energy  $E_0$ , were extracted from the Gd capture data sets using the SAMMY multilevel

TABLE IV

Resonance Energy for Each Sample for Flux Normalization and Normalization Factor Obtained by SAMMY

Sample	Resonance Energy (eV)	Normalization Uncertainty
$^{155}\text{Gd}$	30.047	3.2%
$^{156}\text{Gd}$	33.149	7.8%
$^{157}\text{Gd}$	16.781	1.4%
$^{158}\text{Gd}$	22.295	4.8%
$^{160}\text{Gd}$	222.003	5.7%
$^{nat}\text{Gd}$	16.781	2.5%

R-matrix Bayesian code.<sup>4</sup> The SAMMY code enabled a combined transmission and capture analysis, which employed experimental resolution, Doppler broadening, multiple scattering, and self-shielding. The resolution broadening describes the cumulative effect of the electron burst width in the RPI LINAC, the moderator slowing-down time, the TOF channel width, and the effect of the detector. For capture measurements, the thin capture samples contributed very little to resolution broadening, and thus, this component of broadening was ignored.

A key factor in fitting the correct shape to the experimental data was knowledge of the resolution function, which had a significant impact on the shape-fitting process, especially at epithermal energies. Inaccuracy in the shape of the resolution function can translate into imprecise resonance parameters when fitting experimental data. For this reason, the epithermal capture resolution functions were fit to well-known  $^{238}\text{U}$  resonances using SAMMY. Special attention was given to epithermal energy regions since the resolution function had greater influence in this energy region than in the thermal energy region. The electron burst width and the TOF channel widths were entered as SAMMY input parameters. All remaining resolution function components were described by a Gaussian plus an exponential tail with the energy folding width of 0.06  $\mu\text{s}$  (Ref. 25). This function of magnitude versus time has an integral over time of unity.

As a starting point, the SAMMY code fitted Gd parameters using initial parameters from the previous RPI

experiment<sup>17</sup> in the energy region of 10 to 300 eV and from the ENDF/B-VII.0 evaluation<sup>26</sup> in the energy region above 300 eV. In this experiment, we had five enriched Gd samples and one natural Gd sample. A reduced  $\chi^2$  value was obtained for each Gd sample. The resonance parameters for each Gd sample (isotope) were used as input parameters for the combined fit. Table V shows the reduced  $\chi^2$  value for each step.

As the second step, a combined fit was performed on  $^{nat}\text{Gd}$ ,  $^{155}\text{Gd}$ ,  $^{156}\text{Gd}$ ,  $^{157}\text{Gd}$ ,  $^{158}\text{Gd}$ , and  $^{160}\text{Gd}$  metallic sample data. This was done by fitting each data set sequentially and using the SAMMY parameter file along with the SAMMY covariance matrix file created by the previous fit as input to the next. Resonance parameters of  $^{152}\text{Gd}$  and  $^{154}\text{Gd}$  were fixed to ENDF/B-VII.0 values<sup>26</sup> and not varied for the isotopic samples because of their low abundances (0.2% and 2.18% for natural Gd), but in the case of  $^{154}\text{Gd}$ , we only varied parameters of  $E_0$ ,  $\Gamma_n$ , and  $\Gamma_\gamma$  for the natural sample. When no further improvements in the fit were apparent, and the resonance parameters remained unchanged relative to the previous iteration, the parameters were deemed final. The SAMMY code was then used to calculate capture yield curves based on these final resonance parameters to compare with the experimental data from each Gd sample. The reduced  $\chi^2$  obtained from the second step of the SAMMY fitting is shown in Table V. We also examined each resonance listed in ENDF/B-VII.0 to check whether it was observed in the present data. If it did not look like a resonance peak, we removed the resonance from the parameter file. We fitted several times for each step in order to get the minimum  $\chi^2$  values from the SAMMY fitting. The final reduced  $\chi^2$  values from the SAMMY code are listed in Table V.

The resonance integral  $RI$  was calculated for each Gd isotope using the NJOY code<sup>27</sup> and INTER code.<sup>28</sup> The NJOY code was used to reconstruct room temperature pointwise cross sections given either the ENDF/B-VII.0 or the final Gd resonance parameters, while the INTER code was used to perform the integration to calculate the resonance integral. The resonance integral  $RI$  is defined as follows:

$$RI = \int_{0.5\text{eV}}^{20\text{MeV}} \sigma_\gamma(E) \frac{dE}{E}, \quad (2)$$

TABLE V

Reduced  $\chi^2$  Value for Each Step of the SAMMY Fitting\*

	$^{155}\text{Gd}$	$^{156}\text{Gd}$	$^{157}\text{Gd}$	$^{158}\text{Gd}$	$^{160}\text{Gd}$	$^{nat}\text{Gd}$
First step	3.18	2.88	3.43	2.88	3.78	2.36
Second step	2.49	2.61	2.19	2.67	3.72	1.74
Final step	2.40	2.57	1.97	2.65	3.71	1.64

\*The reduced  $\chi^2$  value means the minimum value obtained by several fittings in each step.

where

$RI$  = infinitely dilute capture resonance integral (b)

$\sigma_\gamma(E)$  = neutron capture cross section generated by NJOY with Gd resonance parameters (b)

$E$  = neutron energy (eV).

The resonance integrals were calculated from 0.5 eV to 20 MeV. The calculation was performed with the present resonance parameters replacing the ENDF/B-VII.0 parameters<sup>26</sup> for all resonances between 21 eV and 1 keV and using the previous RPI resonance parameters<sup>17</sup> for all resonances from 0.2 to 21 eV.

## V. RESULTS

### V.A. Resonance Parameters

The neutron width  $\Gamma_n$ , radiation width  $\Gamma_\gamma$ , and resonance energy  $E_0$  were extracted from the capture yields of five enriched Gd isotopes using the SAMMY version 8.0 multilevel R-matrix Bayesian code.<sup>4</sup> The combined fit employed the experimental resolution and Doppler broadening, self-shielding, and multiple-scattering features of SAMMY. Figure 1 shows data from the natural Gd sample and five enriched isotopic samples as well as the corresponding curves for these data obtained using the SAMMY program. The resulting resonance parameters and the uncertainties of each Gd isotope are presented in Table VI along with evaluated parameters from ENDF/B-VII.0 (Ref. 26) and the previous RPI measurement.<sup>17</sup> The resonance parameters of ENDF/B-VII.1 (Ref. 29) are the same as those of ENDF/B-VII.0 except for 0.032-eV resonance. In Table VI we interpreted the neutron widths of the resonances previously identified by RPI using the present measured isotope and  $J$  value;  $J$  is the total angular momentum of the compound state (also known as the spin state of the resonance) in units of  $h/2\pi$ , where  $h$  is Planck's constant.

The unassigned neutron widths in the previous RPI measurement<sup>17</sup> were treated as  $2ag\Gamma_n$  for odd-A isotopes and  $ag\Gamma_n$  for even-A isotopes, where  $a$  is abundance and  $g$  is the statistical weighting factor:  $g = (2J + 1)/[2(2I + 1)]$ , where  $I$  is the spin of the target nucleus and  $J$  is the total angular momentum of the compound state.

For very low-energy resonances, where the resolution width is minimal, the radiation width  $\Gamma_\gamma$  can be derived directly from the measured data. At higher energy, radiation widths can be determined whenever a resonance includes a significant quantity of scattering. A criterion of  $\Gamma_\gamma/\Gamma_n < 5$  was chosen in Ref. 25 to reflect sensitivity of a resonance to the value of the radiation width. Whenever  $\Gamma_\gamma/\Gamma_n < 5$ , radiation widths were extracted from the data. But, for resonances whose  $\Gamma_\gamma/\Gamma_n$  ratio was  $> 5$ , the experiment effectively measured only the quantity  $\Gamma_n$ . For these mostly capture resonances, neither transmission nor capture data contain sufficient radiation width information.

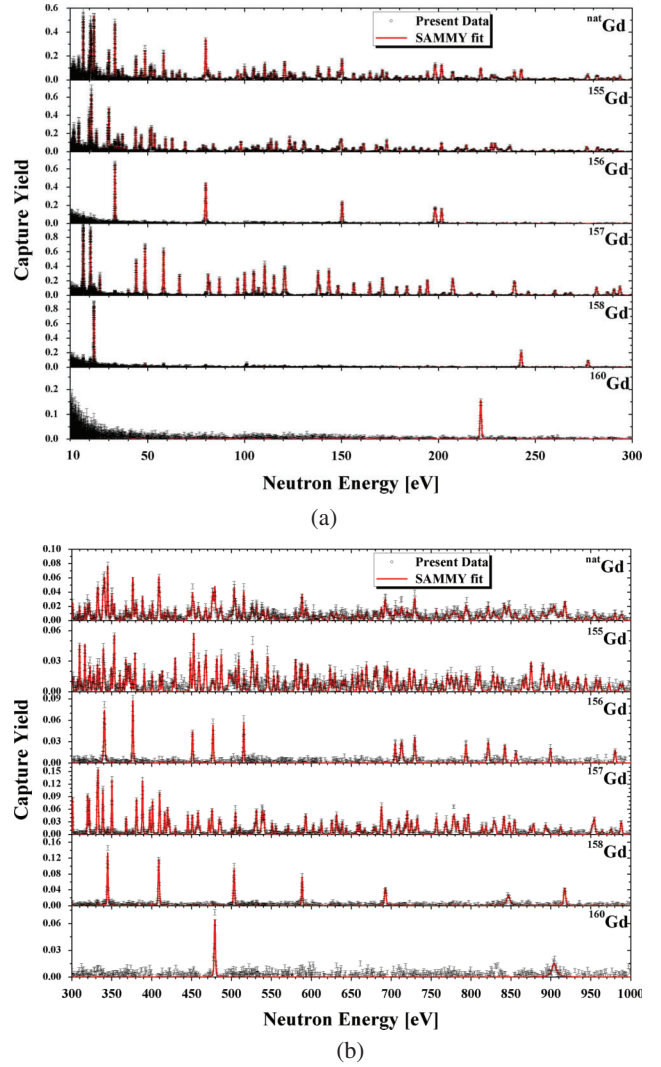


Fig. 1. Capture yield data and calculated fitting curves using resonance parameters obtained with the SAMMY program in the neutron energy region (a) from 10 to 300 eV and (b) from 300 to 1000 eV.

These resonances were assigned the radiation width from ENDF/B-VII.0. New resonances seen in the data but not present in ENDF/B-VII.0 were assigned an average radiation width that was determined by the following method. Resonances sensitive to the value of the radiation width were identified for each isotope; orbital angular momentum; and, where data were available, spin (total angular momentum). Resonances were chosen to use in the determination of the average radiation width  $\langle \Gamma_\gamma \rangle$  if they met the following two criteria:

1. The ENDF/B-VII.0 capture-to-scattering ratio  $\Gamma_\gamma/\Gamma_n$  was  $< 5$ .
2. The resonance was not a minor member of a multiplet, i.e., a shoulder on a larger resonance.

TABLE VI

Resonance Parameters for  $^{152}\text{Gd}$ ,  $^{154}\text{Gd}$ ,  $^{155}\text{Gd}$ ,  $^{156}\text{Gd}$ ,  $^{157}\text{Gd}$ ,  $^{158}\text{Gd}$ , and  $^{160}\text{Gd}$  Isotopes Compared with ENDF/B-VII.0 and Previous RPI Data

Present	RPI	ENDF	$\Gamma_\gamma$ (meV)			$\Gamma_n$ (meV)			Isotope			$J$ Value	
			Present	Source	RPI	ENDF	Present	RPI	ENDF	A	Present	RPI	ENDF
Gadolinium-152													
-6.2	-1	-6.2	55	ENDF	58.6	55	308	4.65	4.516	152	0.5	0.5	0.5
12.35	12.35	12.35	55	RPI	58.6	55	87	84	4.65	152	0.5	0.5	0.5
36.86	36.86	36.86	55	ENDF	56	55	39	39	87	152	0.5	0.5	0.5
39.3	39.3	39.3	55	ENDF	56	55	3.1	3.06	3.1	152	0.5	0.5	0.5
42.73	42.73	42.73	55	ENDF	56	50	60	60	60	152	0.5	0.5	0.5
74.34	74.34	74.34	50	ENDF	50.4	50	3.6	5.11	3.6	152	0.5	0.5	0.5
85.55	85.55	85.55	55	ENDF	58.6	55	87	142	87	152	0.5	0.5	0.5
92.4	92.4	92.4	79	ENDF	58.6	79	124	78.8	124	152	0.5	0.5	0.5
140	140	140	55	ENDF	58.6	55	2.9	2.83	2.9	152	0.5	0.5	0.5
160	160	160	55	ENDF	58.6	55	86	86	86	152	0.5	0.5	0.5
173.8	173.8	173.8	30	ENDF	30.1	30	86	86	86	152	0.5	0.5	0.5
185.7	185.7	185.7	53	ENDF	52.5	53	84	84	84	152	0.5	0.5	0.5
203.1	203.1	203.1	59	ENDF	58.8	59	97	97	97	152	0.5	0.5	0.5
207.7	207.7	207.7	55	ENDF	64.2	64	301	301	301	152	0.5	0.5	0.5
223.3	223.3	223.3	64	ENDF	62	62	46	46	46	152	0.5	0.5	0.5
231.4	231.4	231.4	62	ENDF	100	89.7	300	223.6	300	152	0.5	0.5	0.5
238	238	238	90	ENDF	52.4	53	127	127	127	152	0.5	0.5	0.5
252.4	252.4	252.4	53	ENDF	49.1	49	145	145	145	152	0.5	0.5	0.5
282.6	282.6	282.6	49	ENDF	71	71	352	352	352	152	0.5	0.5	0.5
293.4	293.4	293.4	71	ENDF	55	55	18	18	18	152	0.5	0.5	0.5
303.1	303.1	303.1	55	ENDF	55	55	8.3	8.3	8.3	152	0.5	0.5	0.5
309.5	309.5	309.5	55	ENDF	55	55	65	65	65	152	0.5	0.5	0.5
318.3	318.3	318.3	55	ENDF	55	55	33	33	33	152	0.5	0.5	0.5
333.7	333.7	333.7	55	ENDF	60	60	317	317	317	152	0.5	0.5	0.5
379.2	379.2	379.2	60	ENDF	63	63	180	180	180	152	0.5	0.5	0.5
385.9	385.9	385.9	63	ENDF	53	53	152	152	152	152	0.5	0.5	0.5
405.6	405.6	405.6	53	ENDF	63	419	419	419	419	152	0.5	0.5	0.5
425.7	425.7	425.7	63	ENDF	55	55	29	29	29	152	0.5	0.5	0.5
440.8	440.8	440.8	55	ENDF	55	44	49	49	49	152	0.5	0.5	0.5
472.6	472.6	472.6	55	ENDF	44	44	157	157	157	152	0.5	0.5	0.5
479.4	479.4	479.4	44	ENDF	55	55	14	14	14	152	0.5	0.5	0.5
502	502	502	55	ENDF	55	55	3.4	3.4	3.4	152	0.5	0.5	0.5
505.8	505.8	505.8	55	ENDF	55	55	93	93	93	152	0.5	0.5	0.5
511.7	511.7	511.7	55	ENDF	55	55	49	49	49	152	0.5	0.5	0.5
537.4	537.4	537.4	55	ENDF	55	55	(Continued)						

TABLE VI (Continued)

Present	RPI	ENDF	$\Gamma_\gamma$ (meV)			$\Gamma_n$ (meV)			Isotope			$J/V$ value	
			Present	Source	RPI	ENDF	Present	RPI	ENDF	A	Present	RPI	ENDF
Gadolinium-152													
545.8		545.8	55	ENDF	55	56	55	299	3.7	152	0.5	0.5	0.5
553.2		553.2	56	ENDF	55	55	6	299	152	0.5	0.5	0.5	0.5
558.5		558.5	55	ENDF	67	866	866	6	152	0.5	0.5	0.5	0.5
575.4		575.4	67	ENDF	55	83	83	83	152	0.5	0.5	0.5	0.5
608.3		608.3	55	ENDF	57	276	276	152	152	0.5	0.5	0.5	0.5
619.4		619.4	57	ENDF	55	4.6	4.6	152	152	0.5	0.5	0.5	0.5
626.7		626.7	55	ENDF	55	36	36	152	152	0.5	0.5	0.5	0.5
631.2		631.2	55	ENDF	50	291	291	152	152	0.5	0.5	0.5	0.5
660.3		660.3	50	ENDF	55	750	750	152	152	0.5	0.5	0.5	0.5
683.8		683.8	55	ENDF	55	14	14	152	152	0.5	0.5	0.5	0.5
720.7		720.7	55	ENDF	55	86	86	152	152	0.5	0.5	0.5	0.5
737.8		737.8	55	ENDF	55	13	13	152	152	0.5	0.5	0.5	0.5
751.6		751.6	55	ENDF	55	55	55	152	152	0.5	0.5	0.5	0.5
776.2		776.2	55	ENDF	55	5.9	5.9	152	152	0.5	0.5	0.5	0.5
779.6		779.6	55	ENDF	55	3.6	3.6	152	152	0.5	0.5	0.5	0.5
798		798	55	ENDF	59	242	242	152	152	0.5	0.5	0.5	0.5
805.5		805.5	59	ENDF	54	136	136	152	152	0.5	0.5	0.5	0.5
814.3		814.3	54	ENDF	55	30	30	152	152	0.5	0.5	0.5	0.5
819.6		819.6	55	ENDF	55	37	37	152	152	0.5	0.5	0.5	0.5
830		830	55	ENDF	68	441	441	152	152	0.5	0.5	0.5	0.5
838.2		838.2	68	ENDF	55	44	44	152	152	0.5	0.5	0.5	0.5
883		883	55	ENDF	55	69	69	152	152	0.5	0.5	0.5	0.5
892.3		892.3	55	ENDF	55	79	164	164	152	0.5	0.5	0.5	0.5
910.2		910.2	79	ENDF	79	164	164	152	152	0.5	0.5	0.5	0.5
910.6		910.6	79	ENDF	79	53	53	152	152	0.5	0.5	0.5	0.5
928.8		928.8	55	ENDF	55	123	123	152	152	0.5	0.5	0.5	0.5
948.9		948.9	55	ENDF	55	7.1	7.1	152	152	0.5	0.5	0.5	0.5
956		956	55	ENDF	55	29	29	152	152	0.5	0.5	0.5	0.5
968.5		968.5	55	ENDF	55	145	145	152	152	0.5	0.5	0.5	0.5
972.8		972.8	55	ENDF	56	288	288	152	152	0.5	0.5	0.5	0.5

(Continued)

TABLE VI (Continued)

Present	Energy (eV)	$\Gamma_\gamma$ (meV)				$\Gamma_n$ (meV)				Iso-top			
		RPI	ENDF	Present	$\Gamma_\gamma$ Source	RPI	ENDF	Present	RPI	ENDF	A	Present	RPI
Gadolinium-154													
-2.2	-3	-2.2	74	ENDF	88	74	2	3.55	2	154	0.5	0.5	0.5
11.57 ± 0.05	11.57 ± 0.05	11.58	90 ± 80	RPI	90 ± 80	74	0.2 ± 0.2	0.2 ± 0.2	0.4	154	0.5	0.5	0.5
22.50 ± 0.01	22.5 ± 0.2	22.33	74	ENDF	100 ± 100	74	1.7 ± 1	20 ± 10	12	154	0.5	0.5	0.5
47.14 ± 0.05	47.18 ± 0.04	47.07	88	ENDF	89 ± 8	88	3.9 ± 0.4	2.4 ± 0.6	3.2	154	0.5	0.5	0.5
49.71 ± 0.08	49.63 ± 0.07	49.5	88	ENDF	90 ± 40	88	1.9 ± 0.2	3 ± 1	1.8	154	0.5	0.5	0.5
65.20 ± 0.02	65.21 ± 0.01	65.06	65 ± 6	FIT	100 ± 20	57	30 ± 2	32 ± 5	24	154	0.5	0.5	0.5
75.99 ± 0.15	76.00 ± 0.03	76.12	88	ENDF	90 ± 50	88	1.1 ± 0.1	2.0 ± 0.9	1.1	154	0.5	0.5	0.5
100.66 ± 0.03	100.72 ± 0.08	100.7	83 ± 8	FIT	90 ± 40	82	41 ± 3	48 ± 7	32	154	0.5	0.5	0.5
105.88 ± 0.12	106.05 ± 0.08	105.6	88	ENDF	110 ± 20	88	6 ± 1	11 ± 2	4.8	154	0.5	0.5	0.5
124.18 ± 0.03	124.25 ± 0.08	124	69 ± 6	FIT	110 ± 50	85	103 ± 9	150 ± 20	124	154	0.5	0.5	0.5
139.26 ± 0.03	138.9 ± 0.2	139.2	95 ± 8	FIT	94 ± 8	91	141 ± 12	40 ± 10	124	154	0.5	0.5	0.5
148.5 ± 0.1	148.2 ± 0.2	148.4	83 ± 8	FIT	120 ± 20	88	29 ± 3	46 ± 10	38	154	0.5	0.5	0.5
164.89 ± 0.05	164.8 ± 0.2	164.5	90 ± 8	FIT	98 ± 7	77	117 ± 11	158 ± 2	105	154	0.5	0.5	0.5
170.5 ± 0.2	170.4 ± 0.1	170.4	88	ENDF	85 ± 9	88	5.1 ± 0.5	4.9 ± 0.4	5	154	0.5	0.5	0.5
189.09 ± 0.11	189.30 ± 0.06	New	75	AVG	100 ± 80	New	21 ± 2	14 ± 5	New	154	0.5	0.5	0.5
201.4 ± 0.2	199.5 ± 0.2	201.6	88	ENDF	60 ± 40	88	13 ± 1	80 ± 50	12	154	0.5	0.5	0.5
211.43 ± 0.10	211.57 ± 0.02	211	87 ± 9	FIT	99 ± 8	88	33 ± 3	45 ± 1	35	154	0.5	0.5	0.5
224.10 ± 0.15	224.90 ± 0.02	224	86 ± 9	FIT	100 ± 100	88	18 ± 2	110 ± 60	18	154	0.5	0.5	0.5
235.89 ± 0.10	235.9 ± 0.2	New	75	AVG	70 ± 60	New	41 ± 4	64 ± 9	New	154	0.5	0.5	0.5
252.85 ± 0.21	253.25 ± 0.03	252.8	88	ENDF	101 ± 9	88	12 ± 1	26 ± 1	12	154	0.5	0.5	0.5
257.68 ± 0.10	258.01 ± 0.01	257.5	93 ± 9	FIT	91 ± 7	88	40 ± 4	40 ± 1	34	154	0.5	0.5	0.5
269.40 ± 0.07	269.57 ± 0.03	269.2	91 ± 9	FIT	120 ± 20	88	33 ± 3	30 ± 10	28	154	0.5	0.5	0.5
331.7 ± 0.3	331.7	88	ENDF	88	88	14 ± 1	13.2 ± 1.3	14	154	0.5	0.5	0.5	
333.5 ± 0.3	333.8	88	ENDF	88	88	8.7 ± 0.9	8	154	0.5	0.5	0.5	0.5	
365.3 ± 0.3	364.8	88	ENDF	88	88	102 ± 10	93	154	0.5	0.5	0.5	0.5	
396.9 ± 0.1	396.5	71 ± 7	FIT	65	101 ± 10	94	154	0.5	0.5	0.5	0.5	0.5	0.5
407.3 ± 0.1	407.6	88 ± 9	FIT	88	45 ± 4	44	154	0.5	0.5	0.5	0.5	0.5	0.5
445.2 ± 0.2	444.7	80 ± 8	FIT	76	124 ± 12	120	154	0.5	0.5	0.5	0.5	0.5	0.5
447.0 ± 0.2	447.1	76 ± 7	FIT	69	102 ± 10	93	154	0.5	0.5	0.5	0.5	0.5	0.5
467.7 ± 0.2	468	78 ± 8	FIT	86	115 ± 12	123	154	0.5	0.5	0.5	0.5	0.5	0.5
486.38 ± 0.08	486.77	76 ± 8	FIT	75	60.3 ± 6.0	60	154	0.5	0.5	0.5	0.5	0.5	0.5
491.72 ± 0.46	491.89	73.9	ENDF	73.9	5.3 ± 0.5	5.3	154	0.5	0.5	0.5	0.5	0.5	0.5
512.2 ± 0.2	511.9	89 ± 9	FIT	83	98 ± 10	91	154	0.5	0.5	0.5	0.5	0.5	0.5
516.8 ± 0.2	516.7	85 ± 8	FIT	80	50 ± 5	44	154	0.5	0.5	0.5	0.5	0.5	0.5
552.28 ± 0.29	552.26	71 ± 7	FIT	66	52.7 ± 5.3	47	154	0.5	0.5	0.5	0.5	0.5	0.5
565.6 ± 0.4	565.5	73.9	ENDF	73.9	12 ± 1	12	154	0.5	0.5	0.5	0.5	0.5	0.5

(Continued)

TABLE VI (Continued)

Present	RPI	ENDF	$\Gamma_\gamma$ (meV)			$\Gamma_n$ (meV)			Isotope			$J$ Value		
			Present	RPI	ENDF	Source	$\Gamma_\gamma$	ENDF	Present	RPI	ENDF	A	Present	RPI
Gadolinium-154														
590.68 $\pm$ 0.27	590.51	590.51	66 $\pm$ 6	FIT	FIT	62	159 $\pm$ 16		155	154	0.5		0.5	
593.12 $\pm$ 0.45	593.29	593.29	73.9 $\pm$ 7.4	FIT	FIT	73.9	16 $\pm$ 2		16	154	0.5		0.5	
605.18 $\pm$ 0.49	605.28	605.28	73.9	ENDF	FIT	73.9	3.1 $\pm$ 0.3		3.1	154	0.5		0.5	
625.29 $\pm$ 0.34	626.07	626.07	60 $\pm$ 6	FIT	FIT	62	234 $\pm$ 23		237	154	0.5		0.5	
641.27 $\pm$ 0.23	640.81	640.81	73.6 $\pm$ 7.4	FIT	FIT	73.9	43 $\pm$ 4		43	154	0.5		0.5	
652.4 $\pm$ 0.5	652.4	652.4	73.9	ENDF	FIT	73.9	9.9 $\pm$ 1.0		9.9	154	0.5		0.5	
684.18 $\pm$ 0.38	685.27	685.27	75 $\pm$ 7	FIT	FIT	74	27.4 $\pm$ 2.8		26.7	154	0.5		0.5	
687.44 $\pm$ 0.42	687.95	687.95	74 $\pm$ 7	FIT	FIT	74	40 $\pm$ 4		40	154	0.5		0.5	
696.45 $\pm$ 0.53	696.78	696.78	73.9	ENDF	FIT	73.9	11.6 $\pm$ 1.2		11.6	154	0.5		0.5	
721.85 $\pm$ 0.54	721.81	721.81	73.9	ENDF	FIT	73.9	14.1 $\pm$ 1.4		14.4	154	0.5		0.5	
749.36 $\pm$ 0.52	749.22	749.22	74.1 $\pm$ 7.4	FIT	FIT	73.9	29.0 $\pm$ 2.9		28.8	154	0.5		0.5	
774.36 $\pm$ 0.11	774.89	774.89	58 $\pm$ 6	FIT	FIT	58	103 $\pm$ 10		103	154	0.5		0.5	
796.02 $\pm$ 0.18	795.91	795.91	74.1 $\pm$ 7.4	FIT	FIT	73.9	39 $\pm$ 4		39	154	0.5		0.5	
810.54 $\pm$ 0.50	809.78	809.78	64 $\pm$ 6	FIT	FIT	65	198 $\pm$ 20		199	154	0.5		0.5	
812.37 $\pm$ 0.55	812.46	812.46	74.4 $\pm$ 7.4	FIT	FIT	73.9	55 $\pm$ 5		54	154	0.5		0.5	
837.16 $\pm$ 0.50	837.35	837.35	84 $\pm$ 8	FIT	FIT	74	557 $\pm$ 56		541	154	0.5		0.5	
847.7 $\pm$ 0.6	846.3	846.3	75 $\pm$ 7	FIT	FIT	73	288 $\pm$ 29		286	154	0.5		0.5	
859.65 $\pm$ 0.36	859.97	859.97	78 $\pm$ 7	FIT	FIT	72	328 $\pm$ 33		321	154	0.5		0.5	
880.17 $\pm$ 0.63	880.22	880.22	74.2 $\pm$ 7.4	FIT	FIT	73.9	24 $\pm$ 2		24	154	0.5		0.5	
897.59 $\pm$ 0.62	898.12	898.12	66 $\pm$ 7	FIT	FIT	66	323 $\pm$ 32		323	154	0.5		0.5	
911.15 $\pm$ 0.59	911.48	911.48	73 $\pm$ 7	FIT	FIT	72	73 $\pm$ 7		72	154	0.5		0.5	
917.9 $\pm$ 0.7	917.8	917.8	74 $\pm$ 7	FIT	FIT	75	418 $\pm$ 42		417	154	0.5		0.5	
930.55 $\pm$ 0.49	929.22	929.22	74 $\pm$ 7	FIT	FIT	73	21 $\pm$ 2		21	154	0.5		0.5	
966.90 $\pm$ 0.20	967.77	967.77	70 $\pm$ 7	FIT	FIT	68	275 $\pm$ 27		272	154	0.5		0.5	
973.96 $\pm$ 0.68	973.94	973.94	73.8 $\pm$ 7.4	FIT	FIT	73.9	38 $\pm$ 4		38	154	0.5		0.5	
985.6 $\pm$ 0.6	986.2	986.2	73 $\pm$ 7	FIT	FIT	74	156 $\pm$ 16		157	154	0.5		0.5	

(Continued)

TABLE VI (Continued)

Present	Energy (eV)			$\Gamma_\gamma$ (meV)			$\Gamma_n$ (meV)			Iso-top			$J$ Value
	RPI	ENDF	Present	$\Gamma_\gamma$ Source	RPI	ENDF	Present	RPI	ENDF	A	Present	RPI	ENDF
Gadolinium-155													
0.025±0.003	0.025±0.003	0.0268	104±3	RPI	104±3	108	0.097±0.003	0.097±0.003	0.104	1.55	2	2	2
2.0120±0.0002	2.0120±0.0002	2.008	128±1	RPI	128±1	110	0.40±0.01	0.40±0.01	0.37	1.55	1	1	1
2.5729±0.0003	2.5729±0.0003	2.568	107.1±0.4	RPI	107.1±0.4	111	1.706±0.003	1.706±0.003	1.744	1.55	2	2	2
3.616±0.003	3.616±0.003	3.616	130	RPI	130	0.05±0.02	0.05±0.02	0.04	1.55	1	1	1	
6.3057±0.0002	6.3057±0.0002	6.3	108.8±0.6	RPI	108.8±0.6	114	2.20±0.01	2.20±0.01	2	1.55	2	2	2
7.7477±0.0004	7.7477±0.0004	7.75	109±1	RPI	109±1	124	1.16±0.01	1.16±0.01	1.12	1.55	2	2	2
9.991±0.003	9.991±0.003	10.01	110±20	RPI	110±20	115	0.20±0.04	0.20±0.04	0.17	1.55	2	2	2
11.508±0.001	11.508±0.001	11.53	120±40	RPI	120±40	125	0.78±0.08	0.78±0.08	0.6	1.55	1	1	1
11.964±0.008	11.964±0.008	11.99	130±20	RPI	130±20	112	1.12±0.04	1.12±0.04	0.88	1.55	2	2	2
14.476±0.009	14.476±0.009	14.51	130±10	RPI	130±10	103	3.43±0.09	3.43±0.09	3.2	1.55	1	1	1
17.729±0.005	17.729±0.005	17.77	130±40	RPI	130±40	120	0.47±0.04	0.47±0.04	0.39	1.55	2	2	2
19.86±0.01	19.86±0.01	19.92	118±6	RPI	118±6	104	4.5±0.1	4.5±0.1	4.6	1.55	2	2	2
20.97±0.02	20.97±0.02	21.03	140±20	RPI	140±20	98	11.6±0.5	11.6±0.5	1.55	1.55	2	2	2
22.32±0.01	New	127	New	New	New	New	0.54±0.04	New	1.55	1	New	New	New
23.592±0.003	23.60±0.02	23.67	120	ENDF	140±10	120	2.86±0.06	2.91±0.08	3.12	1.55	2	2	2
27.482±0.007	27.509±0.002	27.57	125	ENDF	140±20	125	1.27±0.06	1.31±0.04	1.12	1.55	1	1	1
29.519±0.003	29.50±0.02	29.58	108	ENDF	113±2	108	4.8±0.1	4.8±0.1	4.32	1.55	2	2	2
30.047±0.002	30.05±0.02	30.1	100	ENDF	130±10	100	11.0±0.2	11.1±0.5	10.4	1.55	2	2	2
31.629±0.008	31.66±0.01	31.72	118	ENDF	140±20	118	1.10±0.05	1.24±0.07	1.12	1.55	2	2	2
33.01±0.01	33.1±0.2	33.14	110	ENDF	110±30	110	1.6±0.1	1.6±0.6	1.87	1.55	1	1	1
33.42±0.01	33.4±0.3	33.51	115	ENDF	120±90	115	1.9±0.1	1±4	1.6	1.55	1	1	1
34.730±0.004	34.73±0.02	34.83	152	ENDF	131±4	152	6.3±0.2	6.8±0.2	6.13	1.55	1	1	1
35.37±0.01	35.39±0.01	35.47	118	ENDF	140±10	118	2.01±0.06	2.17±0.06	1.84	1.55	2	2	2
37.039±0.004	37.066±0.003	37.12	101	ENDF	139±6	101	8.0±0.2	8.3±0.3	8.4	1.55	1	1	1
38.93±0.01	38.93±0.01	39	118	ENDF	130±60	118	1.20±0.06	1.25±0.07	1.04	1.55	2	2	2
43.838±0.003	43.83±0.07	43.92	136	ENDF	140±90	136	16.5±0.3	18±9	17.3	1.55	1	1	1
45.96±0.01	45.98±0.02	46.1	126	ENDF	128±6	126	2.2±0.1	2.3±0.1	2.24	1.55	2	2	2
46.770±0.004	46.79±0.02	46.87	100	ENDF	140±30	100	5.4±0.1	10.2±0.4	5.36	1.55	2	2	2
47.522±0.032	47.628±0.006	47.73	110	ENDF	107±10	110	0.63±0.05	0.39±0.03	0.653	1.55	1	1	1
51.252±0.004	51.25±0.03	51.38	110	ENDF	130±30	110	18.7±0.4	20.3±0.6	18.7	1.55	1	1	1
52.008±0.003	52.01±0.03	52.13	115	ENDF	140±20	115	20.4±0.4	20.9±0.8	19.5	1.55	1	1	1
52.87±0.02	52.89±0.02	53.03	110	ENDF	80±30	110	1.1±0.1	1.2±0.2	1.36	1.55	2	2	2
53.600±0.004	53.62±0.02	53.74	92	ENDF	140±30	92	8.0±0.2	8.7±0.2	7.68	1.55	2	2	2
56.05±0.01	56.12±0.01	56.22	120	ENDF	120±40	120	2.1±0.2	2.5±0.1	2.16	1.55	2	2	2

(Continued)

TABLE VI (Continued)

Present	Energy (eV)			$\Gamma_\gamma$ (meV)			$\Gamma_n$ (meV)			Iso-top	$J$ Value		
	RPI	ENDF	Present	$\Gamma_\gamma$ Source	RPI	ENDF	Present	RPI	ENDF	A	Present	RPI	ENDF
Gadolinium-155													
59.263 ± 0.004	59.30 ± 0.01	59.32	129	ENDF	140 ± 40	129	6.7 ± 0.7	6.9 ± 0.4	6.64	155	2	2	2
62.710 ± 0.004	62.73 ± 0.02	62.84	90	ENDF	150 ± 30	90	7.5 ± 0.8	8.5 ± 0.5	8	155	2	2	2
64.824 ± 0.042	64.028 ± 0.006	64.09	110	ENDF	110 ± 40	110	0.44 ± 0.04	0.49 ± 0.05	0.256	155	2	2	2
66.6 ± 0.1	66.4 ± 0.5	65.2	110	ENDF	120 ± 10	109.8	0.5 ± 0.1	0.5 ± 0.4	1.33	155	1	1	1
68.81 ± 0.03	New	133	New	AVG	New	0.56 ± 0.05	New	12 ± 4	6.32	155	2	2	2
69.42 ± 0.01	69.4 ± 0.1	69.4	110	ENDF	100 ± 100	110	6 ± 1	3.0 ± 0.3	1.6	155	2	2	2
76.74 ± 0.02	76.85 ± 0.01	77	110	ENDF	110 ± 60	110	1.9 ± 0.2	0.9 ± 0.1	1.2	155	1	1	1
77.53 ± 0.06	77.63 ± 0.01	77.8	110	ENDF	110 ± 20	110	1.0 ± 0.1	4.4 ± 0.4	4.2	155	2	2	2
78.69 ± 0.01	78.75 ± 0.06	78.8	110	ENDF	110 ± 30	110	0.9 ± 0.1	8 ± 1	0.312	155	2	2	2
80.63 ± 0.04	80 ± 1	80.1	110	ENDF	112 ± 4	110	0.9 ± 0.1	0 ± 3	2.4	155	1	1	1
80.75 ± 0.05	80.9 ± 0.3	80.9	110	ENDF	110 ± 30	110	1.1 ± 0.1	1.44 ± 0.09	1.1	155	1	1	1
83.91 ± 0.01	83.97 ± 0.02	84.2	110	ENDF	120 ± 40	110	10.6 ± 1.1	10.3 ± 0.1	9.2	155	1	1	1
84.87 ± 0.02	84.91 ± 0.01	85	110	ENDF	110 ± 40	110	3.7 ± 0.4	2.2 ± 0.3	3.1	155	1	1	1
90.30 ± 0.03	90.51 ± 0.02	90.5	110	ENDF	110 ± 90	110	1.4 ± 0.1	2.5 ± 0.2	1.28	155	2	2	2
92.32 ± 0.03	92.47 ± 0.02	92.5	110	ENDF	110 ± 20	110	2.11 ± 0.15	2.14 ± 0.06	2.16	155	2	2	2
92.81 ± 0.02	92.90 ± 0.03	92.8	110	ENDF	110 ± 50	110	2.78 ± 0.28	3.48 ± 0.07	3.12	155	2	2	2
93.91 ± 0.06	93.99 ± 0.01	94.1	110	ENDF	110 ± 40	110	0.58 ± 0.06	0.64 ± 0.09	0.544	155	2	2	2
95.68 ± 0.02	95.70 ± 0.03	95.7	110	ENDF	110 ± 50	110	3.8 ± 0.4	7.1 ± 0.4	3.84	155	2	2	2
96.34 ± 0.01	96.4 ± 0.2	96.6	110	ENDF	110 ± 50	110	7.3 ± 0.7	3.8 ± 0.7	6.26	155	1	1	1
98.22 ± 0.01	98.30 ± 0.03	98.3	110	ENDF	150 ± 20	110	20.0 ± 2.0	11.7 ± 0.4	17.3	155	1	1	1
100.11 ± 0.03	99.9 ± 0.1	100.2	105 ± 10	FIT	110 ± 10	110	2.8 ± 0.2	2.5 ± 0.2	2.13	155	1	1	1
101.27 ± 0.03	101.42 ± 0.02	101.4	110	ENDF	140 ± 30	110	2.2 ± 0.2	2.1 ± 0.2	2.72	155	2	2	2
101.89 ± 0.04	102.03 ± 0.03	102.1	110	ENDF	110 ± 50	110	2.22 ± 0.22	1.52 ± 0.06	1.73	155	1	1	1
104.30 ± 0.01	104.36 ± 0.09	104.4	110	ENDF	110 ± 80	110	10 ± 1	5 ± 1	9	155	1	1	1
105.83 ± 0.02	105.8 ± 0.1	105.9	110	ENDF	140 ± 20	110	7 ± 1	6 ± 1	6.13	155	1	1	1
107.03 ± 0.01	107.14 ± 0.04	107.1	110	ENDF	110 ± 80	110	7 ± 1	9 ± 2	6.24	155	2	2	2
109.46 ± 0.02	109.37 ± 0.02	109.6	110	ENDF	115 ± 2	110	4.0 ± 0.4	7.3 ± 0.5	4.7	155	1	1	1
112.30 ± 0.01	112.40 ± 0.04	112.4	84	ENDF	90 ± 70	84	9.0 ± 0.9	9.1 ± 0.2	9	155	2	2	2
113.71 ± 0.01	113.81 ± 0.05	113.8	132 ± 13	FIT	130 ± 20	67	17 ± 2	20 ± 1	15.2	155	2	2	2
116.46 ± 0.01	116.56 ± 0.06	116.5	116	ENDF	120 ± 80	116	24 ± 2	21 ± 1	17.33	155	1	1	1
116.79 ± 0.06	New	127	New	AVG	New	New	1.2 ± 0.1	New	1.2 ± 0.1	155	1	New	2
118.58 ± 0.04	118.66 ± 0.02	118.6	110	ENDF	110 ± 50	110	1.6 ± 0.2	2.5 ± 0.4	2	155	2	2	2
123.29 ± 0.01	123.35 ± 0.05	123.4	184 ± 18	FIT	200 ± 100	159	44 ± 4	40 ± 6	36	155	1	1	1
124.38 ± 0.02	124.49 ± 0.03	124.4	110	ENDF	120 ± 20	110	5 ± 1	4 ± 1	6.64	155	2	2	2
126.01 ± 0.01	126.11 ± 0.02	126	110	ENDF	110 ± 60	110	27.0 ± 2.7	14.6 ± 0.4	20.5	155	1	1	1

(Continued)

TABLE VI (Continued)

Present	Energy (eV)		$\Gamma_\gamma$ (meV)			$\Gamma_n$ (meV)			Isotope		$J$ Value		
	RPI	ENDF	Present	Source	RPI	ENDF	Present	RPI	ENDF	A	Present	RPI	ENDF
Gadolinium-155													
128.33 ± 0.08	128.53 ± 0.02	129	110	ENDF	110 ± 30	110	1.0 ± 0.1	1.7 ± 0.2	1.12	155	2	2	2
129.71 ± 0.03	129.82 ± 0.01	129.8	110	ENDF	110 ± 40	110	3.3 ± 0.3	3.4 ± 0.3	2.56	155	2	2	2
130.64 ± 0.01	130.79 ± 0.01	130.8	124 ± 12	FIT	150 ± 30	110	34 ± 3	22 ± 3	48.53	155	1	1	1
131.21 ± 0.02	131.37 ± 0.01	New	127	AVG	130 ± 10	New	15.1 ± 1.0	11.4 ± 0.7	New	155	1	Unassigned	New
132.90 ± 0.03	133.04 ± 0.01	133	110	ENDF	140 ± 20	110	4.6 ± 0.5	5.3 ± 0.4	3.73	155	1	1	1
133.77 ± 0.03	133.95 ± 0.01	133.8	110	ENDF	110 ± 30	110	2.9 ± 0.3	3.4 ± 0.2	2.3	155	2	2	2
134.73 ± 0.08	135.13 ± 0.02	134.7	110	ENDF	110 ± 60	110	0.9 ± 0.1	1.9 ± 0.1	0.88	155	2	2	2
137.72 ± 0.02	137.99 ± 0.08	137.8	110	ENDF	120 ± 80	110	18 ± 2	90 ± 30	21.3	155	1	1	1
138.34 ± 0.03	New	New	127	AVG	New	New	2.7 ± 0.2	New	New	155	1	New	New
140.36 ± 0.03	140.55 ± 0.05	140.4	110	ENDF	130 ± 10	110	5.1 ± 0.5	4.9 ± 0.3	4.13	155	1	1	1
141.37 ± 0.04	141.30 ± 0.01	141.4	110	ENDF	120 ± 10	110	1.58 ± 0.16	1.69 ± 0.08	1.04	155	2	2	2
145.52 ± 0.02	145.66 ± 0.01	145.6	110	ENDF	150 ± 20	110	6.1 ± 0.6	6.5 ± 0.3	6.16	155	2	2	2
146.83 ± 0.03	147.02 ± 0.01	146.9	110	ENDF	130 ± 10	110	4.0 ± 0.4	5.3 ± 0.2	3.8	155	2	2	2
148.06 ± 0.02	148.4 ± 0.3	148.2	110	ENDF	110 ± 10	110	9.2 ± 0.9	8.6 ± 0.9	9.6	155	2	2	2
149.36 ± 0.02	149.53 ± 0.03	149.6	150 ± 15	FIT	110 ± 40	110	32 ± 3	36 ± 2	33.33	155	1	1	1
150.01 ± 0.01	150.37 ± 0.04	150.2	147 ± 10	FIT	110 ± 40	110	25 ± 3	80 ± 30	24.8	155	2	2	2
152.22 ± 0.02	152.27 ± 0.01	152.2	110	ENDF	150 ± 40	110	11.0 ± 1.1	6.2 ± 0.8	8	155	1	1	1
153.60 ± 0.07	153.80 ± 0.05	154	110	ENDF	160 ± 30	110	1.3 ± 0.1	1.1 ± 0.2	1.12	155	2	2	2
156.19 ± 0.02	156.4 ± 0.1	156.3	110	ENDF	110 ± 80	110	8 ± 1	30 ± 10	7.68	155	2	2	2
159.98 ± 0.01	160.03 ± 0.07	160.1	110	ENDF	110 ± 50	110	9.7 ± 1.0	10.3 ± 0.5	9.6	155	2	2	2
161.49 ± 0.01	161.57 ± 0.08	161.6	110	ENDF	150 ± 20	110	18.9 ± 1.9	21.6 ± 0.8	20	155	2	2	2
168.17 ± 0.01	168.20 ± 0.09	168.3	123 ± 12	FIT	123 ± 6	110	31 ± 3	31 ± 4	30.13	155	1	1	1
170.23 ± 0.02	170.2 ± 0.1	170.3	110	ENDF	80 ± 30	110	10 ± 1	8 ± 1	8.32	155	2	2	2
171.15 ± 0.02	171.6 ± 0.1	171.4	110	ENDF	110 ± 60	110	9 ± 1	18 ± 1	9.2	155	2	2	2
173.43 ± 0.01	173.5 ± 0.1	173.5	114 ± 11	FIT	110 ± 80	110	32 ± 3	33 ± 2	32.8	155	2	2	2
175.28 ± 0.05	175.46 ± 0.05	175.6	110	ENDF	110 ± 40	110	2.3 ± 0.2	4.2 ± 0.6	2.08	155	2	2	2
177.82 ± 0.02	177.99 ± 0.02	178	110	ENDF	130 ± 10	110	13 ± 1	13 ± 2	9.73	155	1	1	1
180.21 ± 0.02	180.34 ± 0.04	180.4	110	ENDF	110 ± 40	110	17.0 ± 1.7	9.7 ± 0.3	14.7	155	1	Unassigned	New
183.21 ± 0.02	183.20 ± 0.05	New	127	AVG	110 ± 40	New	10.4 ± 0.6	11.7 ± 1.8	New	155	1	Unassigned	New
185.18 ± 0.06	185.11 ± 0.04	New	133	AVG	110 ± 60	New	2.3 ± 0.2	3.2 ± 0.5	New	155	2	Unassigned	New
187.09 ± 0.03	187.36 ± 0.07	New	127	AVG	100 ± 100	New	26.0 ± 1.2	32 ± 2	New	155	1	Unassigned	New
191.24 ± 0.02	New	127	AVG	New	20.2 ± 1.0	New	20.2 ± 1.0	New	New	155	1	New	New
193.43 ± 0.08	New	127	AVG	New	3.3 ± 0.3	New	16.3 ± 0.8	New	New	155	1	New	New
195.01 ± 0.02	New	127	AVG	New	3.1 ± 0.3	New	3.1 ± 0.3	New	New	155	1	New	New

(Continued)

TABLE VI (Continued)

Present	Energy (eV)			$\Gamma_\gamma$ (meV)			$\Gamma_n$ (meV)			Isotope			$J$ Value				
	RPI	ENDF	Present	Source	$\Gamma_\gamma$	RPI	ENDF	Present	RPI	ENDF	A	Present	RPI	ENDF			
Gadolinium-155																	
201.76 ± 0.01	New	133	AVG	New	133	AVG	New	133	AVG	New	27.1 ± 1.0	New	155	2	New		
207.19 ± 0.09	New	133	AVG	New	133	AVG	120 ± 10	New	133	AVG	2.0 ± 0.2	New	155	2	Unassigned		
209.32 ± 0.04	209.1 ± 0.2	New	133	AVG	140 ± 20	New	133	AVG	140 ± 20	New	7.0 ± 0.5	New	155	2	New		
210.23 ± 0.02	210.32 ± 0.01	New	127	AVG	100 ± 10	New	127	AVG	100 ± 10	New	23.8 ± 1.3	New	155	1	Unassigned		
211.93 ± 0.03	212.32 ± 0.02	New	127	AVG	102 ± 10	New	127	AVG	102 ± 10	New	14.7 ± 0.9	New	155	1	Unassigned		
213.37 ± 0.05	213.68 ± 0.02	New	127	AVG	130 ± 20	New	127	AVG	130 ± 20	New	10.4 ± 0.7	New	155	1	Unassigned		
214.51 ± 0.01	214.77 ± 0.01	New	127	AVG	140 ± 10	New	127	AVG	140 ± 10	New	5.8 ± 0.2	New	155	1	Unassigned		
216.88 ± 0.05	New	127	AVG	New	127	AVG	New	127	AVG	New	9.0 ± 0.6	New	155	1	Unassigned		
218.34 ± 0.03	218.57 ± 0.02	New	127	AVG	New	127	AVG	New	127	AVG	19.1 ± 1.0	New	155	1	Unassigned		
219.98 ± 0.07	New	127	AVG	New	127	AVG	New	127	AVG	New	19.0 ± 0.3	New	155	1	New		
224.78 ± 0.02	New	127	AVG	New	133	AVG	New	100 ± 70	New	127	AVG	5.3 ± 0.4	New	155	1	New	
227.57 ± 0.01	229.52 ± 0.02	New	133	AVG	100 ± 100	New	127	AVG	100 ± 100	New	26.4 ± 1.3	New	155	1	New		
229.32 ± 0.01	230.86 ± 0.05	New	127	AVG	100 ± 90	New	127	AVG	100 ± 90	New	37.0 ± 1.3	New	155	2	Unassigned		
230.40 ± 0.03	232.85 ± 0.01	New	127	AVG	100 ± 100	New	127	AVG	100 ± 100	New	38.7 ± 1.5	New	155	2	Unassigned		
231.68 ± 0.05	New	127	AVG	New	133	AVG	New	127	AVG	New	33 ± 2	New	155	1	Unassigned		
232.72 ± 0.04	232.85 ± 0.01	New	133	AVG	New	127	AVG	New	127	AVG	8.7 ± 0.5	New	155	2	Unassigned		
235.31 ± 0.04	New	127	AVG	New	127	AVG	New	127	AVG	New	12 ± 1	New	155	1	Unassigned		
236.27 ± 0.03	New	127	AVG	New	127	AVG	New	100 ± 100	New	127	AVG	10.0 ± 0.3	31 ± 1	New	155	1	
237.16 ± 0.02	237.3 ± 0.1	New	133	AVG	New	127	AVG	New	100 ± 100	New	127	AVG	22.4 ± 1.4	New	155	1	
243.27 ± 0.05	New	133	AVG	New	127	AVG	New	100 ± 100	New	127	AVG	23.3 ± 1.1	New	155	2	Unassigned	
248.68 ± 0.05	New	127	AVG	New	127	AVG	New	100 ± 100	New	127	AVG	5.0 ± 0.4	New	155	2	Unassigned	
252.43 ± 0.08	New	127	AVG	New	127	AVG	New	100 ± 100	New	127	AVG	8.5 ± 0.7	New	155	1	New	
254.65 ± 0.02	New	127	AVG	New	127	AVG	New	100 ± 100	New	127	AVG	3.9 ± 0.4	New	155	1	New	
258.17 ± 0.05	New	127	AVG	New	127	AVG	New	100 ± 100	New	127	AVG	16.3 ± 1.0	New	155	1	New	
259.14 ± 0.05	259.25 ± 0.02	New	127	AVG	New	127	AVG	New	100 ± 100	New	127	AVG	3.2 ± 0.3	New	155	1	Unassigned
262.08 ± 0.03	262.56 ± 0.01	New	133	AVG	New	127	AVG	New	100 ± 100	New	127	AVG	14 ± 1	New	155	1	Unassigned
264.44 ± 0.05	264.89 ± 0.01	New	127	AVG	New	127	AVG	New	100 ± 100	New	127	AVG	5.3 ± 0.4	New	155	2	Unassigned
268.05 ± 0.05	New	127	AVG	New	127	AVG	New	100 ± 100	New	127	AVG	10.0 ± 0.8	New	155	1	New	
269.18 ± 0.06	New	127	AVG	New	127	AVG	New	100 ± 100	New	127	AVG	12.0 ± 0.9	New	155	1	New	
271.22 ± 0.07	New	127	AVG	New	127	AVG	New	100 ± 100	New	127	AVG	8.9 ± 0.7	New	155	1	New	
272.38 ± 0.06	272.36 ± 0.02	New	127	AVG	New	127	AVG	New	100 ± 100	New	127	AVG	4.3 ± 0.4	New	155	1	Unassigned
276.71 ± 0.02	New	133	AVG	New	127	AVG	New	100 ± 100	New	127	AVG	7.6 ± 0.6	New	155	1	New	
279.15 ± 0.10	279.40 ± 0.03	New	127	AVG	98 ± 10	New	127	AVG	98 ± 10	New	28.6 ± 1.3	New	155	2	Unassigned		
282.30 ± 0.02	284.2 ± 0.1	New	127	AVG	100 ± 30	New	127	AVG	100 ± 30	New	5.6 ± 0.5	New	155	1	Unassigned		
284.19 ± 0.04	285.11 ± 0.05	New	127	AVG	150 ± 40	New	133	AVG	150 ± 40	New	19 ± 2	New	155	1	Unassigned		
											10.4 ± 0.8	New	155	2	Unassigned		

(Continued)

TABLE VI (Continued)

Present	Energy (eV)		$\Gamma_\gamma$ (meV)			$\Gamma_n$ (meV)			Isotope			$J$ Value		
	RPI	ENDF	Present	Source	$\Gamma_\gamma$	RPI	ENDF	Present	RPI	ENDF	A	Present	RPI	ENDF
Gadolinium-155														
287.84 ± 0.03	288.85 ± 0.04	288.99 ± 0.03	New	127	Avg	140 ± 30	New	19.8 ± 1.4	21 ± 3	New	155	1	New	New
291.39 ± 0.12			New	127	Avg	130 ± 30	New	4.0 ± 0.4	22 ± 1	New	155	2	Unassigned	New
292.24 ± 0.04	292.37 ± 0.07	292.37 ± 0.07	New	127	Avg	100 ± 10	New	19.2 ± 1.3	20 ± 2	New	155	1	Unassigned	New
294.45 ± 0.07	295.79 ± 0.08	295.79 ± 0.08	New	127	Avg		New	3.0 ± 0.3	3 ± 1	New	155	2	Unassigned	New
300.5 ± 0.2			New	127	Avg		New	7.2 ± 0.6		New	155	1	Unassigned	New
301.6 ± 0.1			New	127	Avg		New	12.1 ± 1.0		New	155	1	New	New
307.4 ± 0.1			New	127	Avg		New	10.4 ± 0.8		New	155	1	New	New
309.92 ± 0.02			New	127	Avg		New	63 ± 4		New	155	1	New	New
312.0 ± 0.1			New	127	Avg		New	7.5 ± 0.7		New	155	1	New	New
313.8 ± 0.1			New	127	Avg		New	4.5 ± 0.4		New	155	1	New	New
316.59 ± 0.02			New	127	Avg		New	68 ± 4		New	155	1	New	New
321.36 ± 0.05			New	133	Avg		New	8.4 ± 0.6		New	155	2	New	New
322.96 ± 0.04			New	133	Avg		New	15.7 ± 1.0		New	155	2	New	New
326.19 ± 0.03			New	127	Avg		New	14.4 ± 1.1		New	155	1	New	New
327.85 ± 0.02			New	127	Avg		New	19 ± 1		New	155	1	New	New
332.41 ± 0.04			New	133	Avg		New	16.8 ± 1.1		New	155	2	New	New
334.86 ± 0.04			New	133	Avg		New	15.1 ± 1.0		New	155	2	New	New
339.67 ± 0.03			New	133	Avg		New	31 ± 2		New	155	2	New	New
341.4 ± 0.1			New	133	Avg		New	11.4 ± 0.9		New	155	2	New	New
349.6 ± 0.1			New	127	Avg		New	32 ± 2		New	155	1	New	New
352.2 ± 0.1			New	127	Avg		New	24 ± 2		New	155	1	New	New
353.44 ± 0.03			New	133	Avg		New	52 ± 3		New	155	2	New	New
360.3 ± 0.1			New	127	Avg		New	24 ± 2		New	155	1	New	New
364.7 ± 0.1			New	127	Avg		New	13.8 ± 1.1		New	155	1	New	New
367.85 ± 0.04			New	127	Avg		New	53 ± 3		New	155	1	New	New
370.1 ± 0.1			New	127	Avg		New	33 ± 2		New	155	1	New	New
371.4 ± 0.1			New	127	Avg		New	35 ± 3		New	155	1	New	New
373.38 ± 0.04			New	127	Avg		New	40 ± 3		New	155	1	New	New
376.0 ± 0.2			New	127	Avg		New	7.0 ± 0.7		New	155	1	New	New
379.40 ± 0.03			New	133	Avg		New	37 ± 2		New	155	2	New	New
391.01 ± 0.05			New	127	Avg		New	38 ± 3		New	155	1	New	New
400.88 ± 0.06			New	127	Avg		New	27 ± 2		New	155	1	New	New
410.53 ± 0.08			New	127	Avg		New	28 ± 2		New	155	1	New	New

(Continued)

TABLE VI (Continued)

Present	RPI	ENDF	$\Gamma_\gamma$ (meV)			$\Gamma_n$ (meV)			Iso-type	$J$ Value	
			Present	$\Gamma_\gamma$ Source	RPI	ENDF	Present	RPI	ENDF	A	Present
Gadolinium-155											
413.41 ± 0.08	New	127	Avg	New	40 ± 3	New	155	1	New	New	New
427.01 ± 0.14	New	127	Avg	New	17 ± 1	New	155	1	New	New	New
429.7 ± 0.1	New	127	Avg	New	99 ± 7	New	155	1	New	New	New
448.83 ± 0.04	New	127	Avg	New	106 ± 8	New	155	1	New	New	New
452.93 ± 0.03	New	133	Avg	New	126 ± 8	New	155	2	New	New	New
459.15 ± 0.05	New	133	Avg	New	32 ± 2	New	155	2	New	New	New
460.2 ± 0.1	New	127	Avg	New	31 ± 3	New	155	1	New	New	New
466.7 ± 0.1	New	127	Avg	New	51 ± 4	New	155	1	New	New	New
468.26 ± 0.04	New	127	Avg	New	157 ± 13	New	155	1	New	New	New
475.6 ± 0.1	New	133	Avg	New	12.9 ± 1.0	New	155	2	New	New	New
477.9 ± 0.1	New	133	Avg	New	10.3 ± 0.9	New	155	2	New	New	New
481.82 ± 0.04	New	127	Avg	New	145 ± 11	New	155	1	New	New	New
487.50 ± 0.04	New	127	Avg	New	191 ± 15	New	155	1	New	New	New
497.2 ± 0.1	New	127	Avg	New	44 ± 4	New	155	1	New	New	New
500.2 ± 0.1	New	127	Avg	New	4050 ± 240	New	155	1	New	New	New
505.4 ± 0.1	New	127	Avg	New	60 ± 5	New	155	1	New	New	New
509.26 ± 0.04	New	127	Avg	New	113 ± 9	New	155	1	New	New	New
516.0 ± 0.1	New	127	Avg	New	29 ± 2	New	155	1	New	New	New
526.4 ± 0.1	New	133	Avg	New	1488 ± 80	New	155	2	New	New	New
532.3 ± 0.1	New	127	Avg	New	84 ± 6	New	155	1	New	New	New
545.55 ± 0.04	New	127	Avg	New	579 ± 52	New	155	1	New	New	New
553.3 ± 0.1	New	127	Avg	New	45 ± 4	New	155	1	New	New	New
558.1 ± 0.1	New	127	Avg	New	53 ± 4	New	155	1	New	New	New
567.8 ± 0.1	New	127	Avg	New	31 ± 3	New	155	1	New	New	New
580.6 ± 0.1	New	127	Avg	New	525 ± 49	New	155	1	New	New	New
586.1 ± 0.1	New	127	Avg	New	89 ± 7	New	155	1	New	New	New
588.3 ± 0.1	New	127	Avg	New	150 ± 12	New	155	1	New	New	New
592.7 ± 0.1	New	127	Avg	New	35 ± 3	New	155	1	New	New	New
595.7 ± 0.1	New	127	Avg	New	131 ± 11	New	155	1	New	New	New
602.8 ± 0.1	New	127	Avg	New	29 ± 3	New	155	1	New	New	New
605.15 ± 0.05	New	127	Avg	New	42 ± 4	New	155	1	New	New	New
611.3 ± 0.1	New	127	Avg	New	28 ± 3	New	155	1	New	New	New

(Continued)

TABLE VI (Continued)

Present	Energy (eV)			$\Gamma_\gamma$ (meV)			$\Gamma_n$ (meV)			Iso-topc			$J$ Value
	RPI	ENDF	Present	$\Gamma_\gamma$ Source	RPI	ENDF	Present	RPI	ENDF	A	Present	RPI	ENDF
Gadolinium-155													
616.5 ± 0.2	New	127	Avg	New	26 ± 2		New	155		1			
623.8 ± 0.1	New	127	Avg	New	135 ± 12		New	155		1			
627.0 ± 0.2	New	127	Avg	New	40 ± 4		New	155		1			
630.0 ± 0.1	New	127	Avg	New	82 ± 7		New	155		1			
638.01 ± 0.13	New	133	Avg	New	18 ± 2		New	155		2			
640.4 ± 0.2	New	127	Avg	New	37 ± 3		New	155		1			
642.8 ± 0.2	New	127	Avg	New	45 ± 4		New	155		1			
651.7 ± 0.1	New	127	Avg	New	77 ± 7		New	155		1			
658.5 ± 0.1	New	133	Avg	New	41 ± 3		New	155		2			
663.9 ± 0.1	New	127	Avg	New	132 ± 12		New	155		1			
669.4 ± 0.1	New	127	Avg	New	633 ± 61		New	155		1			
679.3 ± 0.1	New	127	Avg	New	100 ± 9		New	155		1			
681.8 ± 0.1	New	127	Avg	New	618 ± 63		New	155		1			
692.4 ± 0.1	New	127	Avg	New	161 ± 14		New	155		1			
695.5 ± 0.1	New	127	Avg	New	534 ± 52		New	155		1			
700.1 ± 0.1	New	127	Avg	New	124 ± 11		New	155		1			
707.76 ± 0.09	New	127	Avg	New	129 ± 11		New	155		1			
716.01 ± 0.19	New	127	Avg	New	51 ± 5		New	155		1			
723.2 ± 0.1	New	127	Avg	New	289 ± 27		New	155		1			
729.1 ± 0.1	New	127	Avg	New	1078 ± 97		New	155		1			
737.0 ± 0.2	New	127	Avg	New	57 ± 5		New	155		1			
743.7 ± 0.1	New	133	Avg	New	41 ± 3		New	155		2			
754.7 ± 0.2	New	127	Avg	New	26 ± 2		New	155		1			
756.9 ± 0.1	New	127	Avg	New	63 ± 6		New	155		1			
764.4 ± 0.1	New	127	Avg	New	50 ± 5		New	155		1			
770.7 ± 0.1	New	127	Avg	New	134 ± 12		New	155		1			
772.6 ± 0.2	New	127	Avg	New	44 ± 4		New	155		1			
775.4 ± 0.1	New	133	Avg	New	46 ± 4		New	155		2			
777.4 ± 0.2	New	127	Avg	New	57 ± 5		New	155		1			
781.4 ± 0.1	New	127	Avg	New	74 ± 7		New	155		1			
783.0 ± 0.2	New	127	Avg	New	49 ± 5		New	155		1			
788.1 ± 0.1	New	127	Avg	New	128 ± 12		New	155		1			
794.9 ± 0.1	New	127	Avg	New	131 ± 12		New	155		1			
807.2 ± 0.1	New	127	Avg	New	460 ± 46		New	155		1			

(Continued)

TABLE VI (Continued)

Present	Energy (eV)			$\Gamma_\gamma$ (meV)			$\Gamma_n$ (meV)			Iso-topc		$J$ Value	
	RPI	ENDF	Present	$\Gamma_\gamma$ Source	RPI	ENDF	Present	RPI	ENDF	A	Present	RPI	ENDF
Gadolinium-155													
811.6 ± 0.1	New	127	AVG	New	726 ± 74		New	155	1	New	New	New	New
828.1 ± 0.1	New	127	AVG	New	1057 ± 102		New	155	1	New	New	New	New
833.5 ± 0.1	New	133	AVG	New	60 ± 5		New	155	2	New	New	New	New
839.8 ± 0.1	New	127	AVG	New	106 ± 10		New	155	1	New	New	New	New
864.9 ± 0.2	New	127	AVG	New	105 ± 10		New	155	1	New	New	New	New
869.1 ± 0.1	New	127	AVG	New	260 ± 26		New	155	1	New	New	New	New
875.66 ± 0.04	New	133	AVG	New	377 ± 34		New	155	2	New	New	New	New
888.1 ± 0.4	New	127	AVG	New	48 ± 5		New	155	1	New	New	New	New
890.5 ± 0.1	New	133	AVG	New	953 ± 90		New	155	2	New	New	New	New
897.7 ± 0.1	New	127	AVG	New	431 ± 41		New	155	1	New	New	New	New
904.3 ± 0.1	New	133	AVG	New	117 ± 10		New	155	2	New	New	New	New
913.15 ± 0.11	New	127	AVG	New	317 ± 31		New	155	1	New	New	New	New
918.7 ± 0.1	New	127	AVG	New	414 ± 41		New	155	1	New	New	New	New
922.1 ± 0.2	New	127	AVG	New	97 ± 9		New	155	1	New	New	New	New
934.3 ± 0.2	New	127	AVG	New	286 ± 27		New	155	1	New	New	New	New
944.2 ± 0.1	New	127	AVG	New	235 ± 22		New	155	1	New	New	New	New
957.13 ± 0.08	New	133	AVG	New	64 ± 6		New	155	2	New	New	New	New
961.88 ± 0.08	New	127	AVG	New	223 ± 21		New	155	1	New	New	New	New
973.4 ± 0.2	New	133	AVG	New	38 ± 3		New	155	2	New	New	New	New
987.1 ± 0.2	New	127	AVG	New	70 ± 7		New	155	1	New	New	New	New
990.6 ± 0.2	New	127	AVG	New	81 ± 8		New	155	1	New	New	New	New

(Continued)

TABLE VI (Continued)

Present	Energy (eV)			$\Gamma_\gamma$ (meV)			$\Gamma_n$ (meV)			Iso-top			$J$ Value			
	RPI	ENDF	Present	Source	$\Gamma_\gamma$	RPI	ENDF	Present	RPI	ENDF	A	Present	RPI	ENDF		
Gadolinium-156																
33.149 ± 0.001	33.14 ± 0.03	33.23	90	Discarded <sup>a</sup>	98 ± 3	90	14.2 ± 0.3	14 ± 2	14.6	156	0.5	0.5	0.5	0.5	0.5	
Discarded <sup>a</sup>	56.8	72.2	Discarded <sup>a</sup>	Discarded <sup>a</sup>	85	85	Discarded <sup>a</sup>	Discarded <sup>a</sup>	0.0065	156	Discarded <sup>a</sup>	1.5	1.5	1.5	1.5	
Discarded <sup>a</sup>	80.04 ± 0.07	80.1	71 ± 7	FIT	80 ± 7	85	78 ± 8	80 ± 20	78.8	156	Discarded <sup>a</sup>	0.5	0.5	0.5	0.5	
80.002 ± 0.002	110.5	110.5	Discarded <sup>a</sup>	140 ± 14	80	80	39 ± 4	23 ± 7	41.7	156	0.5	0.5	0.5	0.5	0.5	
Discarded <sup>a</sup>	150.431 ± 0.005	150.62 ± 0.03	150.4	FIT	80 ± 30	80	246 ± 25	200 ± 100	218	156	0.5	0.5	0.5	0.5	0.5	
198.42 ± 0.01	198.4 ± 0.2	198.5	72 ± 7	FIT	92 ± 4	80	39 ± 4	50 ± 10	72	156	0.5	0.5	0.5	0.5	0.5	
201.82 ± 0.01	201.99 ± 0.01	201.8	80 ± 8	FIT	160 ± 40	80	1.85 ± 0.18	3.25 ± 0.06	3.1	156	0.5	0.5	0.5	0.5	0.5	
245.00 ± 0.09	245.16 ± 0.02	244.9	80	ENDF	98 ± 9	80	Discarded <sup>a</sup>	Discarded <sup>a</sup>	0.095	156	Discarded <sup>a</sup>	1.5	1.5	1.5	1.5	
Discarded <sup>a</sup>	258.3	258.3	Discarded <sup>a</sup>	69 ± 7	FIT	80	591 ± 59	591 ± 59	683	156	0.5	0.5	0.5	0.5	0.5	
340.97 ± 0.02	341	72 ± 7	FIT	80	227 ± 23	227 ± 23	146	146	156	156	0.5	0.5	0.5	0.5	0.5	
376.66 ± 0.02	376.7	85	427.3	ENDF	85	2.8 ± 0.3	2.8 ± 0.3	117	117	156	0.5	0.5	0.5	0.5	0.5	
427.3 ± 0.1	427.3	451.4	40 ± 4	FIT	80	129 ± 13	129 ± 13	120	120	156	0.5	0.5	0.5	0.5	0.5	
451.44 ± 0.03	477.07 ± 0.03	65 ± 6	477	FIT	80	119 ± 12	Discarded <sup>a</sup>	Discarded <sup>a</sup>	1.1	156	Discarded <sup>a</sup>	0.5	0.5	0.5	0.5	
Discarded <sup>a</sup>	481.2	481.2	Discarded <sup>a</sup>	Discarded <sup>a</sup>	80	80	Discarded <sup>a</sup>	Discarded <sup>a</sup>	0.225	156	Discarded <sup>a</sup>	1.5	1.5	1.5	1.5	
Discarded <sup>a</sup>	494.3	494.3	Discarded <sup>a</sup>	64 ± 6	FIT	80	161 ± 16	161 ± 16	145	156	0.5	0.5	0.5	0.5	0.5	
515.65 ± 0.03	515.7	549	Discarded <sup>a</sup>	Discarded <sup>a</sup>	80	Discarded <sup>a</sup>	Discarded <sup>a</sup>	0.225	156	Discarded <sup>a</sup>	1.5	1.5	1.5	1.5	1.5	
Discarded <sup>a</sup>	563.6	563.6	Discarded <sup>a</sup>	606.8	Discarded <sup>a</sup>	79.99	79.99	Discarded <sup>a</sup>	3.6	156	Discarded <sup>a</sup>	0.5	0.5	0.5	0.5	
Discarded <sup>a</sup>	662.7	662.7	Discarded <sup>a</sup>	705.5	69 ± 7	FIT	80	Discarded <sup>a</sup>	3.201	156	Discarded <sup>a</sup>	0.5	0.5	0.5	0.5	
Discarded <sup>a</sup>	713.3	713.3	69 ± 7	71.3	67 ± 7	FIT	80	64 ± 6	4.6	156	Discarded <sup>a</sup>	0.5	0.5	0.5	0.5	
729.7	729.7	729.7	71 ± 7	72.9	56 ± 6	FIT	80	1320 ± 130	77	156	0.5	0.5	0.5	0.5	0.5	
794.11 ± 0.03	794.3	821.9	82 ± 8	821.9	82 ± 8	FIT	80	436 ± 44	300	156	0.5	0.5	0.5	0.5	0.5	
822.0 ± 0.1	842.2	842.2	74 ± 7	842.2	94	94	751 ± 75	107 ± 11	124.998	156	0.5	0.5	0.5	0.5	0.5	
842.81 ± 0.08	854.2	854.2	80.03	ENDF	97	97	2.1 ± 0.2	2.1 ± 0.2	2.1	156	0.5	0.5	0.5	0.5	0.5	
855.8 ± 0.5	856.8	856.8	85 ± 9	85 ± 9	80	80	35 ± 3	35 ± 3	29	156	0.5	0.5	0.5	0.5	0.5	
856.7 ± 0.1	900.1	900.1	58 ± 6	900.1	79	79	148 ± 15	148 ± 15	165	156	0.5	0.5	0.5	0.5	0.5	
900.1 ± 0.1	974	974	Discarded <sup>a</sup>	980.93 ± 0.02	69 ± 7	FIT	85	Discarded <sup>a</sup>	1	156	Discarded <sup>a</sup>	1.5	1.5	1.5	1.5	1.5
980.93 ± 0.02	981.1								128	156	0.5					

(Continued)

TABLE VI (Continued)

Present	Energy (eV)	$\Gamma_\gamma$ (meV)				$\Gamma_n$ (meV)				Iso-top	$J$ Value		
		RPI	ENDF	Present	Source	RPI	ENDF	Present	RPI	ENDF			
Gadolinium-157													
0.032 ± 0.003	0.032 ± 0.003	0.0314	107 ± 3	RPI	107 ± 3	106	0.428 ± 0.004	0.428 ± 0.004	0.47	157	2	2	2
2.8287 ± 0.0003	2.8287 ± 0.0003	2.825	109.7 ± 0.9	RPI	109.7 ± 0.9	97	0.377 ± 0.004	0.377 ± 0.004	0.345	157	2	2	2
16.201 ± 0.005	16.201 ± 0.005	16.24	130 ± 30	RPI	130 ± 30	91	0.44 ± 0.03	0.44 ± 0.03	0.4	157	1	1	1
16.78 ± 0.01	16.78 ± 0.01	16.77	112 ± 7	RPI	112 ± 7	81	13.9 ± 0.5	13.9 ± 0.5	12.8	157	2	2	2
20.51 ± 0.02	20.51 ± 0.02	20.56	106 ± 8	RPI	106 ± 8	88	13.4 ± 0.4	13.4 ± 0.4	11.4	157	2	2	2
21.60 ± 0.01	21.59 ± 0.02	21.65	114	ENDF	80 ± 40	114	0.38 ± 0.02	0.34 ± 0.08	0.38	157	2	2	2
23.27 ± 0.01	23.28 ± 0.03	23.33	121	ENDF	140 ± 30	121	0.78 ± 0.04	1.3 ± 0.3	0.8	157	1	1	1
25.349 ± 0.003	25.35 ± 0.01	25.4	85	ENDF	130 ± 30	85	1.71 ± 0.04	1.99 ± 0.06	1.84	157	2	2	2
40.11 ± 0.01	40.08 ± 0.01	40.17	110	ENDF	120 ± 40	110	1.34 ± 0.06	1.6 ± 0.2	1.3	157	1	1	1
44.104 ± 0.002	44.11 ± 0.04	44.22	96	ENDF	120 ± 70	96	9.9 ± 0.2	9 ± 5	8.96	157	2	2	2
48.685 ± 0.002	48.68 ± 0.03	48.8	108 ± 5	FIT	118 ± 9	90	26.2 ± 0.7	26.7 ± 0.5	24	157	2	2	2
58.252 ± 0.002	58.26 ± 0.03	58.38	117 ± 12	FIT	140 ± 20	101	31.3 ± 3.1	32.0 ± 0.6	28	157	2	2	2
66.479 ± 0.004	66.53 ± 0.01	66.65	95 ± 5	FIT	130 ± 60	67	17.1 ± 0.4	16 ± 2	14.66	157	1	1	1
81.240 ± 0.004	81.30 ± 0.04	81.48	108	ENDF	110 ± 40	108	25 ± 2	24 ± 2	20	157	1	1	1
82.04 ± 0.01	82.10 ± 0.04	82.3	85	ENDF	100 ± 70	85	6.7 ± 0.7	7.1 ± 0.6	6.16	157	2	2	2
87.099 ± 0.004	87.17 ± 0.03	87.46	128	ENDF	140 ± 10	128	11.1 ± 1.1	11.1 ± 0.4	10.2	157	2	2	2
96.488 ± 0.005	96.6 ± 0.1	96.6	110	ENDF	100 ± 40	110	12.6 ± 1.3	22.0 ± 0.4	20.3	157	2	2	2
100.0766 ± 0.004	100.16 ± 0.06	100.2	94	ENDF	100 ± 30	94	51 ± 1	43 ± 1	46.66	157	1	1	1
104.8222 ± 0.004	104.89 ± 0.08	105.3	93 ± 6	FIT	103 ± 2	70	70 ± 4	70 ± 40	57.33	157	1	1	1
107.27 ± 0.01	107.46 ± 0.06	107.7	85	ENDF	120 ± 30	85	5.1 ± 0.2	4 ± 1	5.6	157	2	2	2
110.451 ± 0.004	110.54 ± 0.07	110.5	85	ENDF	140 ± 50	85	64 ± 2	50 ± 20	42.4	157	2	2	2
115.2822 ± 0.004	115.37 ± 0.06	115.4	112	ENDF	140 ± 20	112	22.2 ± 2.2	22.2 ± 0.9	19.2	157	2	2	2
120.7474 ± 0.004	120.83 ± 0.01	120.9	95 ± 9	FIT	130 ± 30	91	170 ± 4	140 ± 40	132	157	2	2	2
135.19 ± 0.05	135.19	85	ENDF	85	85	0.93 ± 0.09	0.93 ± 0.09	0.88	157	2	2	2	
137.96 ± 0.02	137.9	138 ± 5	FIT	100 ± 10	86	30.3 ± 1.2	21 ± 9	47.2	157	2	2	2	
138.1 ± 0.1	138.2 ± 0.2	138.8	108 ± 11	FIT	100 ± 10	86	13 ± 1	49.6	157	1	1	1	
138.81 ± 0.02	139.37 ± 0.05	139.3	85	ENDF	100 ± 70	85	14.3 ± 0.7	40 ± 10	6	157	1	1	2
143.629 ± 0.004	143.75 ± 0.01	143.54	147 ± 15	FIT	130 ± 30	88	54 ± 5	60 ± 10	60	157	2	2	2
148.30 ± 0.01	148.55 ± 0.05	148.4	109 ± 11	FIT	140 ± 30	85	25 ± 3	24 ± 1	24	157	1	1	1
156.47 ± 0.01	156.70 ± 0.02	156.38	112 ± 11	FIT	140 ± 50	91	20 ± 2	13 ± 5	19.76	157	2	2	2
164.77 ± 0.01	165.00 ± 0.09	164.83	95 ± 10	FIT	100 ± 80	100	22 ± 2	23 ± 6	34.27	157	2	2	1
167.84 ± 0.02	168.60 ± 0.04	167.88	85	ENDF	99.95	85	2.4 ± 0.2	3.333	157	1	1	1	1

(Continued)

TABLE VI (Continued)

Energy (eV)			$\Gamma_\gamma$ (meV)			$\Gamma_n$ (meV)			Iso-top						
Present	RPI	ENDF	Present	Source	RPI	ENDF	Present	RPI	ENDF	A	Present	RPI	ENDF		
Gadolinium-157															
169.32 ± 0.03	169.4 ± 0.1	169.5	85	ENDF	90 ± 10	85	3.3 ± 0.3	3.4 ± 0.2	3.28	157	2	2	2	2	
171.24 ± 0.01	171.2 ± 0.2	171.2	110 ± 6	FIT	100 ± 10	85	136 ± 9	120 ± 40	44	157	1	1	1	1	
178.58 ± 0.01	178.73 ± 0.03	178.48	145	ENDF	140 ± 20	145	15.9 ± 1.6	17.0 ± 1.0	16	157	2	2	2	2	
183.86 ± 0.01	183.94 ± 0.07	183.76	110 ± 11	FIT	100 ± 90	85	18 ± 2	34 ± 8	29.33	157	2	2	2	1	
190.62 ± 0.01	190.9 ± 0.1	190.58	114 ± 11	FIT	100 ± 90	85	36 ± 4	60 ± 60	28	157	1	1	1	1	
194.48 ± 0.01	194.6 ± 0.1	194.4	124 ± 12	FIT	110 ± 50	85	44 ± 4	60 ± 80	44.8	157	2	2	2	2	
202.81 ± 0.06	202.69	85	202.69	ENDF	85	9.4 ± 0.9	New	1.88 ± 0.18	8.3 ± 0.3	9.6	157	1	1	1	1
203.32 ± 0.04	203.39 ± 0.02	New	102	AVG	130 ± 10	New	1.88 ± 0.18	8.3 ± 0.3	New	157	1	1	1	1	
205.56 ± 0.04	205.75 ± 0.04	205.35	85	ENDF	110 ± 10	85	2.3 ± 0.2	2.0 ± 0.1	0.976	157	2	2	2	2	
207.47 ± 0.01	206.9	85	206.9	ENDF	85	74.7 ± 4	New	2.0 ± 0.1	1.36	157	2	2	2	2	
208.09 ± 0.02	207.77 ± 0.04	208.5	138 ± 12	FIT	150 ± 20	114	11 ± 1	110 ± 30	108	157	2	2	2	2	
217.01 ± 0.03	217.23 ± 0.01	216.9	85	ENDF	121 ± 9	85	9.4 ± 0.9	19.9 ± 0.9	8	157	1	1	1	1	
218.24 ± 0.17	New	111	AVG	New	New	0.55 ± 0.06	New	0.55 ± 0.06	New	157	2	2	2	2	
220.36 ± 0.08	220.24 ± 0.08	220.65	85	ENDF	150 ± 20	85	3.2 ± 0.2	8.3 ± 0.4	4	157	1	1	1	1	
221.20 ± 0.05	New	102	AVG	New	New	4.7 ± 0.4	New	4.7 ± 0.4	New	157	1	1	1	1	
228.21 ± 0.02	227.91 ± 0.02	228.05	85	ENDF	100 ± 100	85	9 ± 1	52 ± 3	6.56	157	2	2	2	2	
232.9 ± 0.1	New	102	AVG	New	New	1.4 ± 0.1	New	1.4 ± 0.1	New	157	1	1	1	1	
237.97 ± 0.09	New	111	AVG	New	New	2.0 ± 0.2	New	2.0 ± 0.2	New	157	2	2	2	2	
239.38 ± 0.01	239.56 ± 0.03	239.3	89 ± 9	FIT	120 ± 20	85	227 ± 23	250 ± 40	253	157	2	2	2	2	
246.46 ± 0.09	246.80 ± 0.01	244.6	85	ENDF	118 ± 9	85	4.1 ± 0.4	19.8 ± 0.5	4.4	157	1	1	1	1	
246.57 ± 0.02	248.83 ± 0.01	246.39	85	ENDF	120 ± 10	85	7.1 ± 0.5	5.0 ± 0.1	9.28	157	2	2	2	2	
250.27 ± 0.03	250.51 ± 0.02	250.2	85	ENDF	130 ± 10	85	5.8 ± 0.4	8.2 ± 0.2	5.73	157	1	1	1	1	
254.65 ± 0.10	254.87 ± 0.01	255	85	ENDF	130 ± 10	85	2.3 ± 0.2	18.6 ± 0.5	2.2	157	1	1	1	1	
257.00 ± 0.18	256.46 ± 0.06	255.2	85	ENDF	101 ± 10	85	1.84 ± 0.18	1.46 ± 0.18	2.24	157	1	1	1	1	
260.26 ± 0.01	260.53 ± 0.01	260.05	125 ± 10	FIT	120 ± 10	85	30.4 ± 1.3	31 ± 3	21.86	157	1	1	1	1	
265.73 ± 0.02	266.05 ± 0.01	265.8	85	ENDF	110 ± 10	85	6.9 ± 0.4	7.9 ± 0.2	6.4	157	2	2	2	2	
268.29 ± 0.03	268.47 ± 0.01	268.02	85	ENDF	140 ± 20	85	9.2 ± 0.9	17.0 ± 0.9	10.5	157	2	2	2	2	
281.77 ± 0.01	282.28 ± 0.05	281.02	75 ± 8	FIT	110 ± 100	85	43 ± 4	70 ± 30	64	157	2	2	2	2	
287.47 ± 0.03	287.89 ± 0.04	287.6	85	ENDF	100 ± 50	85	13 ± 1	25 ± 3	14	157	2	2	2	2	
290.81 ± 0.02	291.08 ± 0.03	290.8	92 ± 9	FIT	100 ± 50	85	61 ± 6	51 ± 9	65	157	1	1	1	1	
293.82 ± 0.01	294.16 ± 0.01	293.7	89 ± 9	FIT	130 ± 30	85	49 ± 5	49 ± 8	61	157	2	2	2	2	

(Continued)

TABLE VI (Continued)

Energy (eV)			$\Gamma_\gamma$ (meV)			$\Gamma_n$ (meV)			Iso-top			$J$ Value		
Present	RPI	ENDF	Present	Source	RPI	ENDF	Present	RPI	ENDF	A	Present	RPI	ENDF	
Gadolinium-157														
301.09 $\pm$ 0.02	Discarded <sup>b</sup>	300.9	105 $\pm$ 11	FIT	85	64.3 $\pm$ 6.4	53.333	157	1					
319.93 $\pm$ 0.02	Discarded <sup>b</sup>	306.4	Discarded <sup>b</sup>	New	85	Discarded <sup>b</sup>	2.8	157	Discarded <sup>b</sup>					
321.96 $\pm$ 0.02	New	111	Avg	New	39.1 $\pm$ 1.6	New	157	1	2					
331.99 $\pm$ 0.03	New	111	Avg	New	32.6 $\pm$ 1.3	New	157	2	2					
333.08 $\pm$ 0.03	New	102	Avg	New	129 $\pm$ 11	New	157	1	1					
339.10 $\pm$ 0.02	New	111	Avg	New	113 $\pm$ 7	New	157	2	2					
350.46 $\pm$ 0.01	New	102	Avg	New	194 $\pm$ 12	New	157	1	1					
368.26 $\pm$ 0.03	New	102	Avg	New	100 $\pm$ 5	New	157	2	2					
376.4 $\pm$ 0.1	New	102	Avg	New	33 $\pm$ 2	New	157	1	1					
381.30 $\pm$ 0.02	New	102	Avg	New	4.0 $\pm$ 0.4	New	157	1	1					
388.79 $\pm$ 0.02	New	111	Avg	New	223 $\pm$ 18	New	157	1	1					
396.04 $\pm$ 0.12	New	102	Avg	New	166 $\pm$ 10	New	157	2	2					
397.92 $\pm$ 0.01	New	102	Avg	New	5.9 $\pm$ 0.6	New	157	1	1					
401.38 $\pm$ 0.01	New	111	Avg	New	75 $\pm$ 5	New	157	1	1					
410.28 $\pm$ 0.02	New	111	Avg	New	54 $\pm$ 2	New	157	2	2					
416.60 $\pm$ 0.03	New	102	Avg	New	87 $\pm$ 4	New	157	2	2					
420.19 $\pm$ 0.03	New	102	Avg	New	66 $\pm$ 4	New	157	1	1					
422.35 $\pm$ 0.04	New	102	Avg	New	119 $\pm$ 9	New	157	1	1					
430.01 $\pm$ 0.04	New	102	Avg	New	35 $\pm$ 2	New	157	1	1					
445.62 $\pm$ 0.03	New	111	Avg	New	17 $\pm$ 1	New	157	1	1					
451.17 $\pm$ 0.02	New	102	Avg	New	13.7 $\pm$ 1.1	New	157	1	1					
456.1 $\pm$ 0.1	New	102	Avg	New	32 $\pm$ 2	New	157	2	2					
458.27 $\pm$ 0.03	New	102	Avg	New	64 $\pm$ 4	New	157	1	1					
460.4 $\pm$ 0.1	New	102	Avg	New	35 $\pm$ 2	New	157	1	1					
472.00 $\pm$ 0.02	New	102	Avg	New	17 $\pm$ 1	New	157	1	1					
475.87 $\pm$ 0.03	New	102	Avg	New	113 $\pm$ 8	New	157	1	1					
485.00 $\pm$ 0.04	New	102	Avg	New	18 $\pm$ 1	New	157	1	1					
486.8 $\pm$ 0.1	New	102	Avg	New	40 $\pm$ 3	New	157	1	1					
500.6 $\pm$ 0.1	New	102	Avg	New	9.8 $\pm$ 0.9	New	157	1	1					
505.23 $\pm$ 0.03	New	111	Avg	New	44 $\pm$ 2	New	157	2	2					
510.7 $\pm$ 0.1	New	102	Avg	New	18 $\pm$ 1	New	157	1	1					
527.3 $\pm$ 0.2	New	102	Avg	New	8.3 $\pm$ 0.8	New	157	1	1					
529.6 $\pm$ 0.1	New	102	Avg	New	30 $\pm$ 2	New	157	1	1					
531.46 $\pm$ 0.03	New	102	Avg	New	290 $\pm$ 27	New	157	1	1					

(Continued)

TABLE VI (Continued)

Energy (eV)			$\Gamma_\gamma$ (meV)			$\Gamma_n$ (meV)			Iso-top			$J$ Value		
Present	RPI	ENDF	Present	$\Gamma_\gamma$ Source	RPI	ENDF	Present	RPI	ENDF	A	Present	RPI	ENDF	
Gadolinium-157														
538.60 ± 0.03	New	102	AVG	New	744 ± 54	New	157	1	New	157	1	New	New	New
540.94 ± 0.04	New	102	AVG	New	134 ± 12	New	157	1	New	157	2	New	New	New
551.10 ± 0.03	New	111	AVG	New	20 ± 1	New	157	1	New	157	1	New	New	New
555.90 ± 0.02	New	102	AVG	New	25 ± 2	New	157	1	New	157	1	New	New	New
567.9 ± 0.1	New	102	AVG	New	15 ± 1	New	157	1	New	157	1	New	New	New
571.3 ± 0.1	New	102	AVG	New	32 ± 3	New	157	1	New	157	1	New	New	New
584.3 ± 0.1	New	102	AVG	New	25 ± 2	New	157	1	New	157	1	New	New	New
593.26 ± 0.04	New	102	AVG	New	611 ± 51	New	157	1	New	157	1	New	New	New
602.79 ± 0.05	New	111	AVG	New	21 ± 1	New	157	2	New	157	2	New	New	New
610.02 ± 0.08	New	111	AVG	New	9.4 ± 0.8	New	157	2	New	157	2	New	New	New
613.02 ± 0.04	New	111	AVG	New	29 ± 2	New	157	2	New	157	2	New	New	New
626.00 ± 0.04	New	111	AVG	New	36 ± 2	New	157	2	New	157	2	New	New	New
631.85 ± 0.03	New	111	AVG	New	66 ± 4	New	157	2	New	157	2	New	New	New
634.6 ± 0.1	New	111	AVG	New	17 ± 1	New	157	2	New	157	2	New	New	New
639.07 ± 0.05	New	111	AVG	New	31 ± 2	New	157	2	New	157	2	New	New	New
644.0 ± 0.1	New	111	AVG	New	13.6 ± 1.1	New	157	2	New	157	2	New	New	New
658.1 ± 0.1	New	102	AVG	New	53 ± 4	New	157	1	New	157	2	New	New	New
661.1 ± 0.1	New	102	AVG	New	62 ± 5	New	157	1	New	157	1	New	New	New
667.0 ± 0.1	New	102	AVG	New	23 ± 2	New	157	1	New	157	1	New	New	New
678.5 ± 0.1	New	102	AVG	New	37 ± 3	New	157	1	New	157	1	New	New	New
681.0 ± 0.1	New	102	AVG	New	34 ± 3	New	157	1	New	157	2	New	New	New
688.24 ± 0.04	New	111	AVG	New	263 ± 21	New	157	2	New	157	2	New	New	New
696.8 ± 0.1	New	102	AVG	New	107 ± 9	New	157	1	New	157	1	New	New	New
699.0 ± 0.1	New	102	AVG	New	89 ± 8	New	157	1	New	157	2	New	New	New
707.77 ± 0.06	New	111	AVG	New	21 ± 2	New	157	1	New	157	2	New	New	New
710.0 ± 0.1	New	102	AVG	New	133 ± 12	New	157	1	New	157	1	New	New	New
717.5 ± 0.1	New	102	AVG	New	70 ± 6	New	157	1	New	157	1	New	New	New
720.43 ± 0.05	New	111	AVG	New	151 ± 12	New	157	2	New	157	1	New	New	New
725.6 ± 0.1	New	102	AVG	New	172 ± 16	New	157	1	New	157	1	New	New	New
729.6 ± 0.2	New	102	AVG	New	16 ± 2	New	157	1	New	157	1	New	New	New
733.1 ± 0.1	New	102	AVG	New	604 ± 51	New	157	1	New	157	1	New	New	New
756.7 ± 0.1	New	102	AVG	New	62 ± 6	New	157	1	New	157	1	New	New	New
757.4 ± 0.1	New	102	AVG	New	124 ± 12	New	157	1	New	157	1	New	New	New
767.7 ± 0.2	New	102	AVG	New	35 ± 3	New	157	1	New	157	1	New	(Continued)	

TABLE VI (Continued)

Energy (eV)			$\Gamma_\gamma$ (meV)			$\Gamma_n$ (meV)			Iso-top			$J$ Value		
Present	RPI	ENDF	Present	$\Gamma_\gamma$ Source	RPI	ENDF	Present	RPI	ENDF	A	Present	RPI	ENDF	
Gadolinium-157														
769.3 $\pm$ 0.1	New	111	Avg	New	55 $\pm$ 4	New	157	2						
778.82 $\pm$ 0.03	New	111	Avg	New	1895 $\pm$ 114	New	157	2						
783.8 $\pm$ 0.1	New	102	Avg	New	179 $\pm$ 18	New	157	1						
792.32 $\pm$ 0.04	New	111	Avg	New	76 $\pm$ 6	New	157	2						
796.9 $\pm$ 0.1	New	111	Avg	New	179 $\pm$ 15	New	157	2						
814.3 $\pm$ 0.1	New	111	Avg	New	35 $\pm$ 3	New	157	2						
819.1 $\pm$ 0.1	New	111	Avg	New	37 $\pm$ 3	New	157	2						
825.6 $\pm$ 0.2	New	102	Avg	New	26 $\pm$ 3	New	157	1						
829.0 $\pm$ 0.1	New	102	Avg	New	342 $\pm$ 34	New	157	1						
831.0 $\pm$ 0.1	New	102	Avg	New	97 $\pm$ 9	New	157	1						
841.6 $\pm$ 0.1	New	111	Avg	New	153 $\pm$ 12	New	157	2						
848.4 $\pm$ 0.1	New	102	Avg	New	507 $\pm$ 49	New	157	1						
855.0 $\pm$ 0.1	New	111	Avg	New	98 $\pm$ 8	New	157	2						
874.6 $\pm$ 0.1	New	102	Avg	New	71 $\pm$ 7	New	157	1						
878.7 $\pm$ 0.1	New	102	Avg	New	265 $\pm$ 26	New	157	1						
893.83 $\pm$ 0.04	New	111	Avg	New	53 $\pm$ 4	New	157	2						
896.7 $\pm$ 0.2	New	102	Avg	New	49 $\pm$ 5	New	157	1						
912.77 $\pm$ 0.11	New	102	Avg	New	120 $\pm$ 11	New	157	1						
925.6 $\pm$ 0.2	New	102	Avg	New	40 $\pm$ 4	New	157	1						
952.2 $\pm$ 0.2	New	102	Avg	New	106 $\pm$ 12	New	157	1						
954.8 $\pm$ 0.1	New	111	Avg	New	467 $\pm$ 46	New	157	2						
964.6 $\pm$ 0.2	New	111	Avg	New	20 $\pm$ 2	New	157	2						
975.8 $\pm$ 0.3	New	111	Avg	New	31 $\pm$ 3	New	157	2						
988.7 $\pm$ 0.1	New	111	Avg	New	135 $\pm$ 11	New	157	2						

(Continued)

TABLE VI (Continued)

Present	Energy (eV)		$\Gamma_\gamma$ (meV)			$\Gamma_n$ (meV)			Isotope		$J$ Value		
	RPI	ENDF	Present	$\Gamma_\gamma$ Source	RPI	ENDF	Present	RPI	ENDF	A	Present	RPI	ENDF
Gadolinium-158													
-65				-65	90	90	74	74	158	0.5	0.5	0.5	0.5
22.295 ± 0.001	22.30 ± 0.04	22.3	96	ENDF	100 ± 40	96	7.2 ± 0.1	7.1 ± 0.8	158	0.5	0.5	0.5	0.5
101.12 ± 0.01	101.20 ± 0.09	101.1	88	ENDF	120 ± 10	88	1.4 ± 0.1	1.3 ± 0.2	0.85	158	0.5	0.5	0.5
242.87 ± 0.01	243.17 ± 0.01	242.7	132 ± 13	FIT	90 ± 20	105	36 ± 4	50 ± 20	58	158	0.5	0.5	0.5
277.41 ± 0.01	277.38 ± 0.06	277.2	90	ENDF	100 ± 300	90	16 ± 2	40 ± 60	13	158	0.5	0.5	0.5
298.72 ± 0.02	298.0 ± 0.1	New	74	AVG	110 ± 10	New	1.03 ± 0.09	1.5 ± 0.3	New	158	0.5	Unassigned	New
345.08 ± 0.01	344.8	63 ± 6		FIT	93	283 ± 28			157	158	0.5		0.5
409.14 ± 0.02	409.1	73 ± 7		FIT	100	353 ± 35			272	158	0.5		0.5
503.51 ± 0.02	503.3	67 ± 7		FIT	105	353 ± 35			270	158	0.5		0.5
588.78 ± 0.03	588.5	125 ± 12		FIT	112	49 ± 5			57	158	0.5		0.5
693.1 ± 0.1	692.9	58 ± 6		FIT	95	736 ± 74			755	158	0.5		0.5
847.0 ± 0.1	847.3	80 ± 8		FIT	107	2680 ± 270			1700	158	0.5		0.5
Discarded <sup>b</sup>	869.3	Discarded <sup>b</sup>		FIT	88	Discarded <sup>b</sup>			1.6	158	0.5		0.5
917.8 ± 0.1	917.1	84 ± 8		FIT	83	689 ± 69			460	158	0.5		0.5
Gadolinium-160													
-326		-326	88	ENDF	80 ± 20	88	6374	50 ± 20	6374	160	0.5	0.5	0.5
222.00 ± 0.01	222.22 ± 0.03	222	111 ± 11	Discarded <sup>b</sup>		120	48 ± 5	Discarded <sup>b</sup>	50 ± 20	160	0.5	Discarded <sup>b</sup>	0.5
Discarded <sup>b</sup>	421.9	Discarded <sup>b</sup>		FIT		88	Discarded <sup>b</sup>	Discarded <sup>b</sup>	0.75	160	0.5	Discarded <sup>b</sup>	0.5
Discarded <sup>b</sup>	447.9	Discarded <sup>b</sup>				125	457 ± 46	457 ± 46	19	160	0.5	Discarded <sup>b</sup>	0.5
479.37 ± 0.03	478.9	87 ± 9		FIT		88	Discarded <sup>b</sup>	Discarded <sup>b</sup>	345	160	0.5	Discarded <sup>b</sup>	0.5
Discarded <sup>b</sup>	571.8	Discarded <sup>b</sup>				89	Discarded <sup>b</sup>	Discarded <sup>b</sup>	3	160	0.5	Discarded <sup>b</sup>	0.5
Discarded <sup>b</sup>	707.5	Discarded <sup>b</sup>		FIT		105	4570 ± 460	4570 ± 460	1.9	160	0.5	Discarded <sup>b</sup>	0.5
Discarded <sup>b</sup>	752.6	127 ± 13				89	Discarded <sup>b</sup>	Discarded <sup>b</sup>	2.45	160	0.5	Discarded <sup>b</sup>	0.5
904.4 ± 0.2	904.9			FIT					3500	160	0.5		0.5
Discarded <sup>b</sup>	984								4.6	160	0.5		0.5

<sup>a</sup>Only ENDF/B-VII.0.<sup>b</sup>ENDF/B-VI.8 and ENDF/B-VII.0.

Each  $\langle \Gamma_\gamma \rangle$  in Table VII was an inverse-variance weighted average of radiation widths from sensitive resonances. The radiation widths and uncertainties of new resonances in Table VI were assigned  $\langle \Gamma_\gamma \rangle$  and  $\Delta \langle \Gamma_\gamma \rangle$  from Table VII for their radiation widths.

The fifth column in Table VI, labeled “ $\Gamma_\gamma$  Source,” designates whether the  $\Gamma_\gamma$  in Table VI was fitted from the data (FIT), fixed to an average value from Table VII (AVG), fixed to the ENDF/B-VII.0 value (ENDF), or fixed to the previous RPI value (RPI) where the neutron energy was  $< 21$  eV.

Potential sources of uncertainty include the capture flux normalization and the analytical descriptions of the resolution functions. Uncertainties in sample thicknesses given in Table III were not included in the final uncertainties given in Table VI. The resonance parameters for  $^{152}\text{Gd}$  were not fitted because the abundance was very low. In these cases the resonance parameters were assigned ENDF/B-VII.0 values in Table VI without any quoted errors.

Figure 2 shows transmission and capture yield data in the epithermal region for the natural Gd sample and calculated curves using resonance parameters obtained by the SAMMY program. The transmission data in Fig. 2 were taken from the previous RPI measurement.<sup>17</sup> The SAMMY fit in Figs. 2 and 3 is the calculated curve using the resonance parameters obtained from the present data. The present resonance parameters were determined using the capture yields for five enriched Gd isotopic samples and a natural sample. Figure 3 shows transmission data for the natural Gd sample in the neutron energy region from 10 to 300 eV and calculated curves using resonance parameters from the present data, ENDF/B-VII.0 (Ref. 26), and the previous RPI result<sup>17</sup> by using the SAMMY program without fitting. The resonance parameters from the present and the previous RPI data agree with the experimental transmission better than those of ENDF/B-VII.0.

We observed 2, 169, 96, and 1 new resonances not listed in ENDF/B-VII.0 from the  $^{154}\text{Gd}$ ,  $^{155}\text{Gd}$ ,  $^{157}\text{Gd}$ , and  $^{158}\text{Gd}$  isotopes, respectively, as listed in Table VI. Because the present measurements did not support their existence, 11 resonances from the  $^{156}\text{Gd}$  isotope; 1 resonance from the  $^{157}\text{Gd}$  and  $^{158}\text{Gd}$  isotopes, respectively; and 6 resonances from the  $^{160}\text{Gd}$  isotope listed in ENDF/B-VII.0 were discarded. Recently, new measurements of resonance parameters for  $^{155}\text{Gd}$  with the DANCE gamma-ray calorimeter at the LANSCE were presented.<sup>9</sup> Four new resonances identified in Ref. 9 were confirmed in the present results: 22.32, 68.81, 116.79, and 138.34 eV in the  $^{155}\text{Gd}$  isotope. However, the spin assignments for 38 resonances were different from those in ENDF/B-VII.0 or the present result. We checked the present resonance parameters using the spin assignment in Ref. 9, but we could not see any differences. Thus, the determination of  $\Gamma_\gamma$  and  $\Gamma_n$  was not sensitive to the spin assignment.

Fitting results are shown in Fig. 4 with the final resonance parameters in the neutron energy region from 200 to 250 eV, where there are many new resonances listed in Table VI. The data for  $^{nat}\text{Gd}$  were fitted very nicely with the new resonance parameters from the Gd isotopes as shown in Fig. 4. In this energy region, 12 unassigned resonances from the previous RPI measurement in Table VI were identified. Two resonances in ENDF excluded by the previous RPI measurement were identified: 202.81 eV in  $^{157}\text{Gd}$  and 207.47 eV in  $^{157}\text{Gd}$ . The 201.6-eV resonance in  $^{154}\text{Gd}$ , identified by Ref. 10, was reported at 201.4 eV in Table VI, while the previous RPI result showed it at 199.5 eV. A resonance at 202.1 eV in  $^{156}\text{Gd}$  was observed. It had been included in ENDF/B-VI.8 but was excluded from ENDF/B-VII.0. The resolved resonance representation for  $^{155}\text{Gd}$  ends at 180 eV in ENDF/B-VII.0. It was extended to 300 eV by the previous RPI measurement.<sup>17,30</sup> Reference 30 is a comprehensive version of Ref. 17. Twelve new resonances

TABLE VII  
Average Radiation Width  $\langle \Gamma_\gamma \rangle$  for Each Gd Isotope in the Energy Range from 10 to 1000 eV

Gadolinium Isotope	<i>J</i>	Average Radiation Width $\langle \Gamma_\gamma \rangle \pm \Delta \langle \Gamma_\gamma \rangle$ (meV)	Comment
$^{152}\text{Gd}$	0.5	Unknown	No data
$^{154}\text{Gd}$	0.5	$75 \pm 1$	41 resonances
$^{155}\text{Gd}$	1	$127 \pm 12$	5 resonances
$^{155}\text{Gd}$	2	$133 \pm 10$	3 resonances
$^{156}\text{Gd}$	0.5	$65 \pm 4$	18 resonances
$^{157}\text{Gd}$	2	$102 \pm 3$	9 resonances
$^{157}\text{Gd}$	0.5	$111 \pm 6$	13 resonances
$^{158}\text{Gd}$	0.5	$74 \pm 7$	8 resonances
$^{160}\text{Gd}$	0.5	$103 \pm 12$	3 resonances

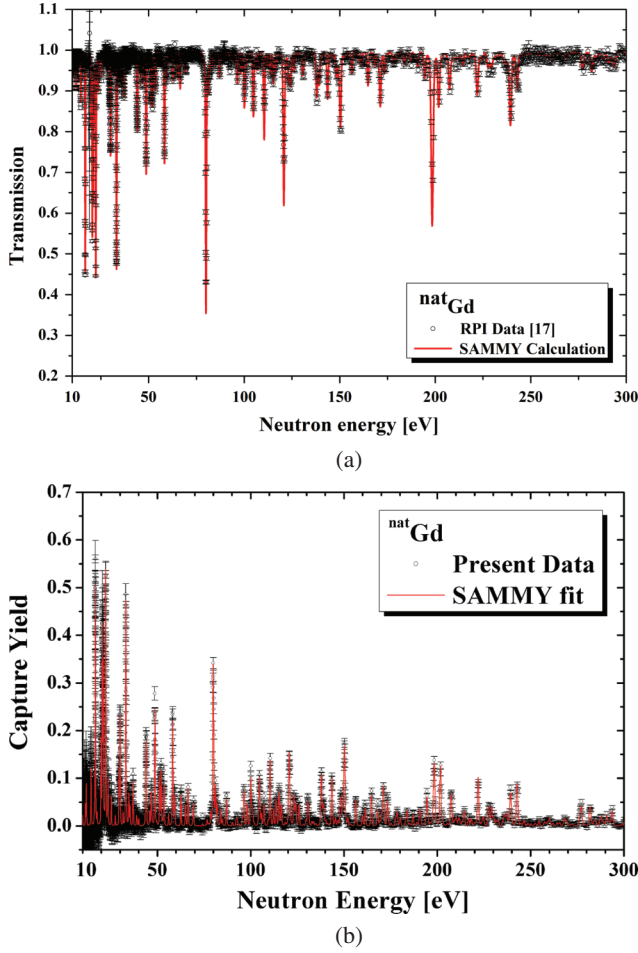


Fig. 2. (a) Transmission data and (b) capture yield for  $^{nat}\text{Gd}$  with a fitting curve using resonance parameters obtained with the SAMMY program.

(201.76, 207.19, 216.88, 218.34, 219.98, 224.78, 227.57, 231.68, 235.31, 236.27, 243.27, and 248.68 eV) in  $^{155}\text{Gd}$  and four new resonances (218.24, 221.20, 232.90, and 237.97 eV) in  $^{157}\text{Gd}$  that were not identified in either ENDF/B-VII.0 or the previous RPI measurement have been added in the 200- to 250-eV region. Among 11 unassigned resonances from the previous RPI measurement, 10 resonances were assigned to the  $^{155}\text{Gd}$  isotope, and 1 resonance at 203.39 eV was identified as  $^{157}\text{Gd}$  at 203.32 eV, as listed in Table VI.

Fitting results in the neutron energy region from 250 to 300 eV are shown in Fig. 5. Ten new resonances from  $^{155}\text{Gd}$  were identified in the 250- to 300-eV regions that were not included in ENDF/B-VII.0 or the previous RPI results. The resonance at 298.0 eV from the previous RPI measurement (with only natural samples) was identified in  $^{158}\text{Gd}$  at 298.7 eV. One resonance at 258.3 eV in  $^{156}\text{Gd}$ , listed in ENDF/B-VII.0, was not seen in the present measurement.

These results have been reviewed at RPI and supersede parameters given in Refs. 17 and 30 from

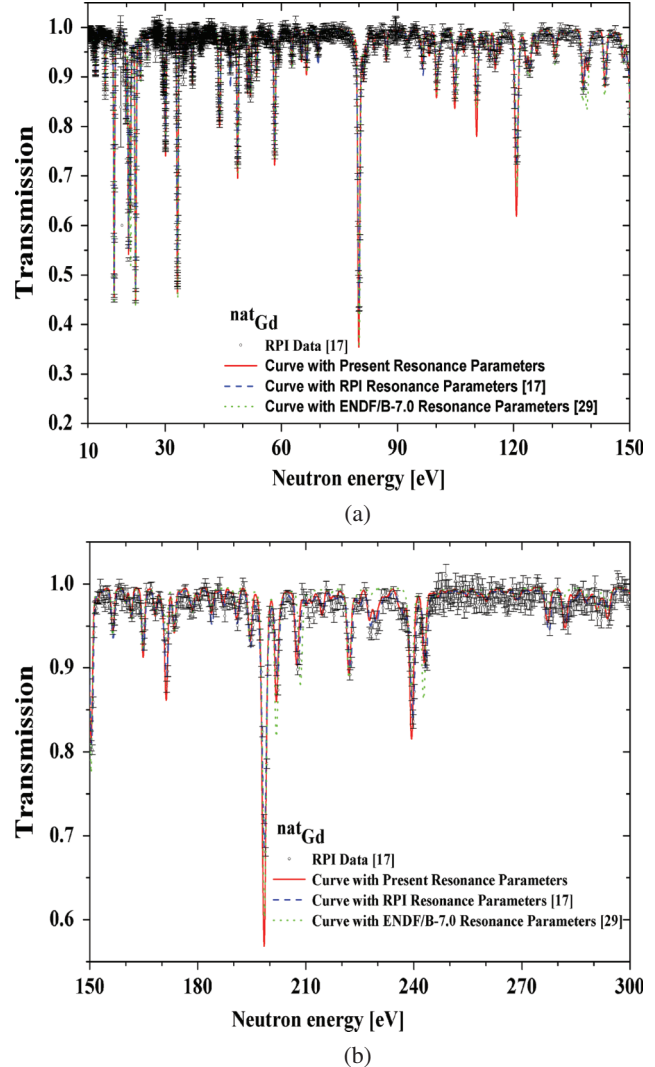


Fig. 3. Transmission of the previous RPI data<sup>17</sup> with curves using resonance parameters from present, RPI (Ref. 17), and ENDF/B-VII.1 (Ref. 29) in the neutron energy region (a) from 10 to 150 eV and (b) from 150 to 300 eV.

measurements of only elemental samples. The previous RPI measurement<sup>17,30</sup> ended at 300 eV. All of the 28 new resonances identified in the previous measurement have been confirmed and assigned to an isotope and a spin state  $J$ . They are included in Table VI.

Above 300 eV, very few measurements are reported.<sup>10,12,14</sup> We identified 116 new resonances from  $^{155}\text{Gd}$  and 90 new resonances from  $^{157}\text{Gd}$  in the 300- to 1000-eV region. Figure 6 includes seven resonances (481.2, 494.3, 549, 563.6, 606.8, 662.7, and 974 eV) from  $^{156}\text{Gd}$ , one resonance (306.4 eV) from  $^{157}\text{Gd}$ , one resonance (869.3 eV) from  $^{158}\text{Gd}$ , and six resonances (421.9, 447.9, 571.8, 707.5, 752.6, and 984 eV) from  $^{160}\text{Gd}$  listed in ENDF/B-VII.0 that have been discarded from the present analysis.

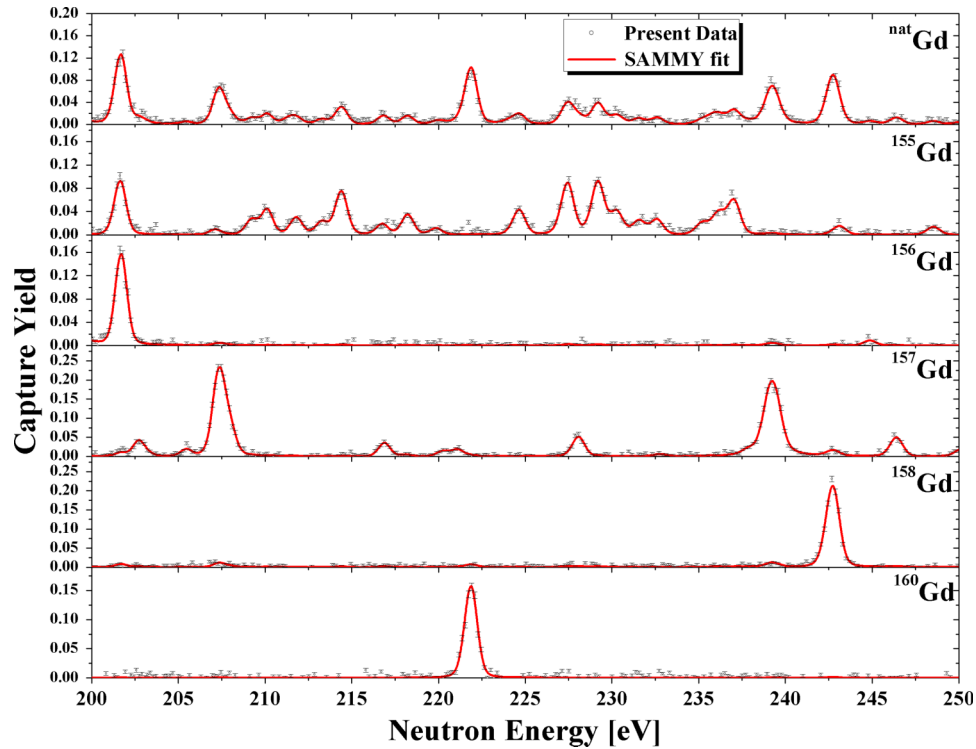


Fig. 4. Capture yield data and calculated fitting curves in the neutron energy region from 200 to 250 eV using the resonance parameters obtained with the SAMMY program.

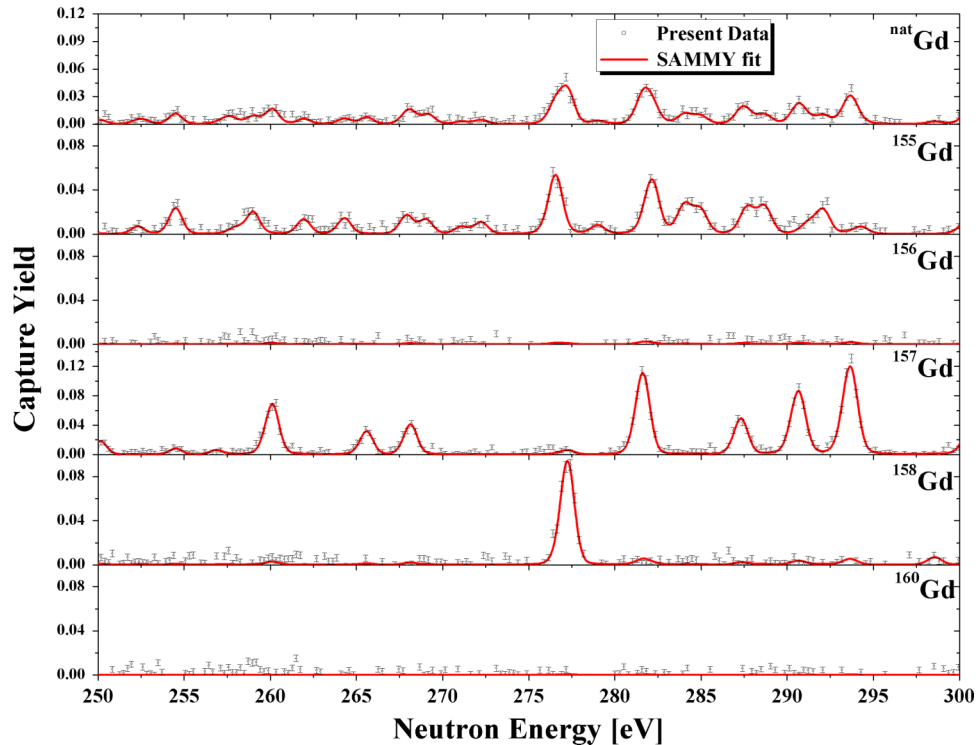


Fig. 5. Capture yield data and calculated fitting curves in the neutron energy region from 250 to 300 eV using the resonance parameters obtained with the SAMMY program.

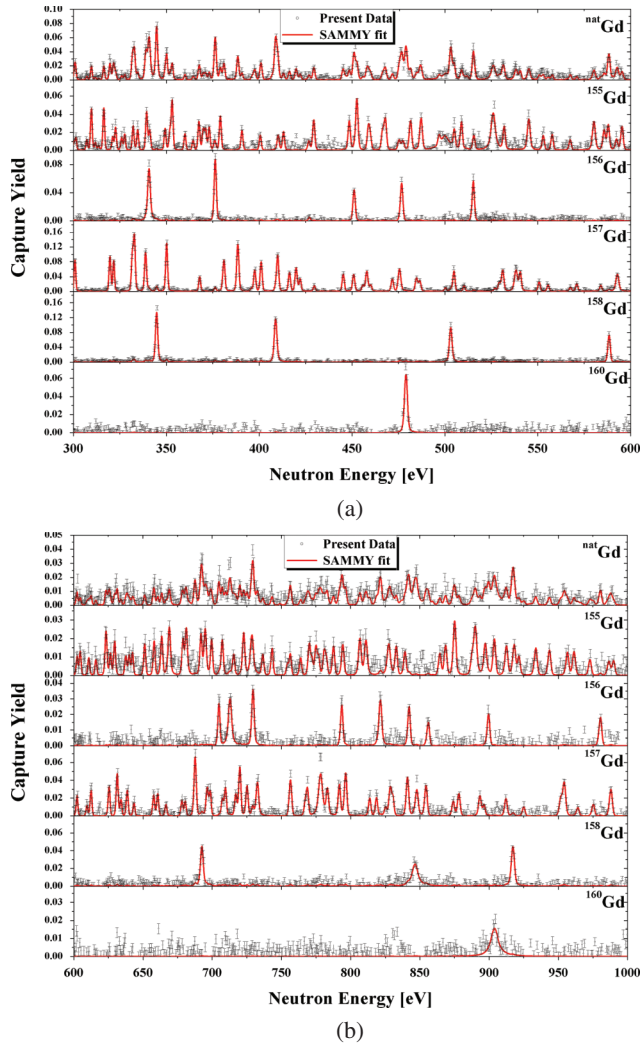


Fig. 6. Capture yield data and calculated fitting curves in the neutron energy region (a) from 300 to 600 eV and (b) from 600 to 1000 eV using the resonance parameters obtained with the SAMMY program.

### V.B. Resonance Integrals

Equation (2) and the resonance parameters listed in Table VI were used to calculate resonance integrals. The resonance integral calculations used resonance parameters from the previous RPI measurement in the energy range 0.02 to 21 eV and from ENDF/B-VII.0 for the negative energy resonances and for the energy region above the present measurement. The resonance integrals were calculated using the NJOY (Ref. 27) and the INTER (Ref. 28) programs. The results are shown in Table VIII in units of barns. The uncertainty in the resonance integrals was calculated by differentiating the resonance integral with respect to resonance parameters according to the error propagation formula and treating  $\sigma_\gamma(E)$  as a sum of single-level Breit-Wigner resonances.<sup>25</sup> The resonance integral of  $^{152}\text{Gd}$  in the RPI column used resonance parameters from ENDF/B-VI.8. The resonance integral of  $^{154}\text{Gd}$  is 16% larger than that calculated from the ENDF/B-VII.0 resonance parameters. The contributions of  $^{155}\text{Gd}$  to the elemental Gd capture resonance integral are more than half, and their contribution is similar to that calculated using the resonance parameters from ENDF/B-VII.0 and RPI. The present parameters gave a resonance integral value of  $395 \pm 2$  b, which is  $\sim 0.8\%$  higher and  $\sim 1.7\%$  lower than that obtained with the ENDF/B-VII.0 parameters and with the previous RPI parameters, respectively.

## VI. CONCLUSIONS

Resonance parameters were extracted from capture data sets for Gd isotopes using the multilevel R-matrix Bayesian code SAMMY. The analysis included Doppler broadening, resolution broadening, and multiple scattering correcting of capture data.

We observed 2, 169, 96, and 1 new resonances from the  $^{154}\text{Gd}$ ,  $^{155}\text{Gd}$ ,  $^{157}\text{Gd}$ , and  $^{158}\text{Gd}$  isotopes, respectively.

TABLE VIII

Calculated Capture Resonance Integrals for Gd Isotopes in the Energy Range from 0.5 eV to 20 MeV

Isotope	Abundance (%)	Capture Resonance Integral (b)			Percent Change (%)	
		Present	ENDF/B-VII.0	RPI	ENDF/B-VII.0	RPI
$^{152}\text{Gd}$	0.20	560	560	476	0	+18
$^{154}\text{Gd}$	2.18	$252 \pm 8$	217	261	+16	-4
$^{155}\text{Gd}$	14.80	$1535 \pm 9$	1539	1570	-0.3	-2.3
$^{156}\text{Gd}$	20.47	$102 \pm 2$	108	104	-6	-2
$^{157}\text{Gd}$	15.65	$776 \pm 6$	753	789	+3	-2
$^{158}\text{Gd}$	24.84	$70 \pm 1$	68	71.5	+3	-2
$^{160}\text{Gd}$	21.86	$7.3 \pm 0.1$	8.2	7.66	-11	-5
$^{nat}\text{Gd}$	—	$395 \pm 2$	392	402	+0.8	-1.7

Because the present measurements did not support their existence, 11 resonances from the  $^{156}\text{Gd}$  isotope, 1 resonance each from the  $^{157}\text{Gd}$  and  $^{158}\text{Gd}$  isotopes, and 6 resonances from the  $^{160}\text{Gd}$  isotope listed in ENDF/B-VII.0 have been discarded.

The resulting resonance parameters were used to calculate the capture resonance integral in the energy region from 0.5 eV to 20 MeV. The capture resonance integrals were compared to the resonance integrals obtained using the resonance parameters from ENDF/B-VII.0 and the previous RPI results. The present parameters gave a resonance integral value of  $395 \pm 2$  b, which is  $\sim 0.8\%$  higher and  $\sim 1.7\%$  lower than that obtained with the ENDF/B-VII.0 parameters and with the previous RPI parameters, respectively.

#### ACKNOWLEDGMENTS

The authors express their sincere thanks to the staff of the Gaerttner Linear Accelerator Center at RPI for their excellent operation and their support during the experiment. This research partly was supported by the National Research Foundation of Korea (NRF) through a grant provided by the Korean Ministry of Science, ICT and Future Planning (MSIP) (NRF-2013R1A2A2A01067340), by the Institutional Activity Program of Korea Atomic Energy Research Institute, and by the National Research and Development Program through the Dong-Nam Institute of Radiological and Medical Sciences funded by MSIP (50491-2014).

#### REFERENCES

1. R. Q. WRIGHT, "Revised Evaluations for ENDF/B-VI Revision 2," *Trans. Am. Nucl. Soc.*, **68**, 468 (1993).
2. K. WISSHAK et al., "Stellar Neutron Capture Cross Sections of the Gd Isotopes," *Phys. Rev. C*, **52**, 2762 (1995); <http://dx.doi.org/10.1103/PhysRevC.52.2762>.
3. Y. NAKAJIMA et al., "Neutron Capture Cross-Section Measurements of  $^{155}\text{Gd}$  and  $^{157}\text{Gd}$  from 1.1 to 235 keV," *Ann. Nucl. Energy*, **16**, 589 (1989); [http://dx.doi.org/10.1016/0306-4549\(89\)90013-3](http://dx.doi.org/10.1016/0306-4549(89)90013-3).
4. N. M. LARSON, "Updated Users' Guide for SAMMY: Multilevel R-Matrix Fits to Neutron Data Using Bayes' Equations," ORNL/TM-9179/R8, ENDF-364/R2, Oak Ridge National Laboratory (2008).
5. S. F. MUGHABGHAB and R. E. CHRIEN, " $s$ -Wave Neutron Strength Functions of the Gd Isotopes," *Phys. Rev.*, **180**, 1131 (1969); <http://dx.doi.org/10.1103/PhysRev.180.1131>.
6. F. B. SIMPSON, "Neutron Resonance Parameters for Sm $^{147}$ , Sm $^{149}$ , Gd $^{155}$ , and Gd $^{157}$ ," *Bull. Am. Phys. Soc.*, **2**, 42 (NAT) (1957).
7. H. B. MØLLER, F. J. SHORE, and V. L. SAILOR, "Low-Energy Neutron Resonances in Erbium and Gadolinium," *Nucl. Sci. Eng.*, **8**, 183 (1960); <http://dx.doi.org/10.13182/NSE60-1>.
8. M. P. FRICKE et al., "Neutron Resonance Parameters and Radiative Capture Cross Section of Gd from 3 eV to 750 keV," *Nucl. Phys. A*, **146**, 337 (1970); [http://dx.doi.org/10.1016/0375-9474\(70\)90729-3](http://dx.doi.org/10.1016/0375-9474(70)90729-3).
9. B. BARAMSAI, "Neutron Capture Reaction on Gadolinium Isotopes," PhD Thesis, North Carolina State University (2010).
10. F. RAHN et al., "Neutron Resonance Spectroscopy:  $^{154,158,160}\text{Gd}$ ," *Phys. Rev. C*, **10**, 1904 (1974); <http://dx.doi.org/10.1103/PhysRevC.10.1904>.
11. V. A. ANUFRIEV, S. I. BABICH, and S. M. MASYONOV, EXFOR/CINDA Database; [www.nndc.bnl.gov](http://www.nndc.bnl.gov), NNDC CINDA EXFOR Accession #40984 (1987) (current as of June 6, 2014).
12. R. L. MACKLIN, "Neutron Capture Resonances of  $^{152}\text{Gd}$  and  $^{154}\text{Gd}$ ," *Nucl. Sci. Eng.*, **95**, 304 (1987); <http://dx.doi.org/10.13182/NSE87-2>.
13. F. N. BELYAEV et al., EXFOR/CINDA Database; [www.nndc.bnl.gov](http://www.nndc.bnl.gov), NNDC CINDA EXFOR Accession #41107 (1990) (current as of June 6, 2014).
14. E. N. KARZHAVINA, N. N. PHONG, and A. B. POPOV, EXFOR/CINDA Database; [www.nndc.bnl.gov](http://www.nndc.bnl.gov), NNDC CINDA EXFOR Accession #40162 (1968) (current as of June 6, 2014).
15. E. N. KARZHAVINA, K.-S. SU, and A. B. POPOV, EXFOR/CINDA Database; [www.nndc.bnl.gov](http://www.nndc.bnl.gov), NNDC CINDA EXFOR Accession #40405 (1973).
16. M. ASGHAR et al., "The Spins of Low-Energy Neutron Resonances of  $^{155}\text{Gd}$  and  $^{157}\text{Gd}$ ," *Nucl. Phys. A*, **145**, 549 (1970); [http://dx.doi.org/10.1016/0375-9474\(70\)90440-9](http://dx.doi.org/10.1016/0375-9474(70)90440-9).
17. G. LEINWEBER et al., "Neutron Capture and Total Cross-Section Measurements and Resonance Parameters of Gadolinium," *Nucl. Sci. Eng.*, **154**, 261 (2006); <http://dx.doi.org/10.13182/NSE05-64>.
18. R. W. HOCKENBURY et al., "Neutron Radiative Capture in Na, Al, Fe, and Ni from 1 to 200 keV," *Phys. Rev.*, **178**, 4, 1746 (1969); <http://dx.doi.org/10.1103/PhysRev.178.1746>.
19. M. E. OVERBERG et al., "Photoneutron Target Development for the RPI Linear Accelerator," *Nucl. Instrum. Methods Phys. Res., Sect. A*, **438**, 253 (1999); [http://dx.doi.org/10.1016/S0168-9002\(99\)00878-5](http://dx.doi.org/10.1016/S0168-9002(99)00878-5).
20. R. E. SLOVACEK et al., "Neutron Cross-Section Measurements at the Rensselaer LINAC," *Proc. Topl. Mtg. Advances in Reactor Physics*, Knoxville, Tennessee, April 11–15, 1994, Vol. II, p. 193, American Nuclear Society (1994).

21. R. C. BLOCK et al., "A Multiplicity Detector for Accurate Low-Energy Neutron Capture Measurements," *Proc. Int. Conf. Nuclear Data for Science and Technology*, Mito, Japan, May 30–June 3, 1998, p. 383 (1998).
22. R. C. BLOCK et al., "Neutron Time-of-Flight Measurements at the Rensselaer LINAC," *Proc. Int. Conf. Nuclear Data for Science and Technology*, Gatlinburg, Tennessee, May 9–13, 1994, Vol. 1, p. 81, American Nuclear Society (1994).
23. G. LEINWEBER et al., "Resonance Parameters and Uncertainties Derived from Epithermal Neutron Capture and Transmission Measurements of Natural Molybdenum," *Nucl. Sci. Eng.*, **164**, 287 (2010); <http://dx.doi.org/10.13182/NSE08-76>.
24. E. M. BAUM et al., "Chart of the Nuclides," 17th ed., Knolls Atomic Power Laboratory (2009).
25. D. P. BARRY, "Neodymium Neutron Transmission and Capture Measurements and Development of a New Transmission Detector," PhD Thesis, Rensselaer Polytechnic Institute (2003).
26. M. B. CHADWICK et al., "ENDF/B-VII.0: Next Generation Evaluated Nuclear Data Library for Science and Technology," *Nucl. Data Sheets*, **107**, 2931 (2006); <http://dx.doi.org/10.1016/j.nds.2006.11.001>.
27. R. E. MacFARLANE and D. W. MUIR, "The NJOY Nuclear Data Processing System Version 91," LA-12740-M, Los Alamos National Laboratory (1994).
28. C. L. DUNFORD, "ENDF Utility Codes Release 7.01/02," USCD1212/07, International Atomic Energy Agency (Apr. 27, 2005).
29. M. B. CHADWICK et al., "ENDF/B-VII.1 Nuclear Data for Science and Technology: Cross Sections, Covariances, Fission Product Yields and Decay Data," *Nucl. Data Sheets*, **112**, 12, 2887 (2011); <http://dx.doi.org/10.1016/j.nds.2011.11.002>.
30. G. LEINWEBER et al., "Neutron Capture and Transmission Measurements and Resonance Parameter Analysis of Gadolinium," OSTI Report No. LM-05K107, U.S. Department of Energy Office of Scientific and Technical Information (2005).